AN OBSERVATIONAL STUDY ON QUANTIFYING THE DISTANCE OF SUPERCELL-BOUNDARY INTERACTION IN THE GREAT PLAINS

by

Kathleen Marie Magee

A thesis submitted to the faculty of
The University of North Carolina at Charlotte
in partial fulfillment of the requirements
for the degree of Master of Science in
Earth Science

Charlotte

2017

Approved by:

_____
Dr. Casey Davenport

_____
Dr. Matthew Eastin

_____
Mr. Terry Shirley

© 2017
Kathleen Marie Magee
ALL RIGHTS RESERVED

ABSTRACT

KATHLEEN MARIE MAGEE. An observational study on quantifying the distance of supercell-boundary interaction in the Great Plains. (Under the direction of DR. CASEY DAVENPORT)

Several case studies and numerical simulations have confirmed that baroclinic boundaries provide enhanced horizontal and vertical vorticity, wind shear, helicity, and moisture that induce stronger updrafts, higher reflectivity, and stronger low-level rotation in supercells. However, the distance at which a boundary will provide such enhancement is less well-defined. Previous studies have identified distances ranging from 5 km to 200 km, and only focused on tornadogenesis rather than all forms of severe weather. To better aid short-term forecasts, the actual distances at which supercells produce severe weather in proximity to a boundary needs to be assessed.

In this study, the distance between a large number of supercells and nearby surface boundaries (including warm fronts, stationary fronts, and outflow boundaries) is measured throughout the lifetime of each storm; the distance at which associated reports of large hail, strong winds, and tornadoes is also collected. Data is gathered from SPC storm reports, WPC surface analyses, ASOS archives, and NCDC radar archives. The Integrated Data Viewer (IDV) from Unidata is used to analyze the distance of the supercell from the boundary every twenty minutes. These distances are then used to interpolate the distance at which severe and significantly severe reports occurred; reports are grouped by severe type (tornado, hail, or wind), then by boundary type (warm front, stationary front, or outflow). Using these distributions, the range from the boundary at

which each type of severe weather is produced is identified per boundary type to assist forecasters.

Overall, the range at which tornadoes are more likely to be produced is generally closer to the boundary than hail and wind reports for all three boundary types, likely owing to the enhanced helicity present near a boundary. Statistical analyses are used to assess the sensitivity of report distributions to report type, boundary type, distance from the boundary, and boundary strength. The distance of different report types near the same boundary surprisingly did not test as statistically different, except for warm fronts; however, when comparing the distances of the same report type associated with different boundaries, statistically significant differences were found for different boundaries in which different report types are maximally produced. Temperature gradients are not as statistically different between boundaries, but the temperature gradient within the same boundary is statistically significant for the occurrence of tornadoes vs. hail.

Additional analyses were conducted to complement the distributions of severe report distances. Previous research has demonstrated that the angle at which supercells interact with boundaries impacts tornado production; in the present dataset, supercells interacting at an angle less than 45° are not only more likely to produce tornadoes, but also more likely to produce significantly severe tornadoes. Additionally, other studies have suggested that the temperature gradient of a boundary is of minimal importance with regards to tornado production. Interestingly, the tornadoes in this study were associated with stronger temperature gradients than for hail or wind production, thus

implying that a stronger amount of baroclinically-generated horizontal vorticity is required for tornadogenesis, likely due to the enhanced low-level rotation.

ACKNOWLEDGEMENTS

I would like to thank Dr. Casey Davenport for continuous support of my research and creating a supportive and encouraging graduate school experience. Thank you to my committee for working with me to produce the best research possible. Also, thank you to the severe storms research group for the additional insight, informal therapy sessions, and additional revisions and analyses. Lastly, thank you to my family and friends for all of your love and support throughout these very formative years.

TABLE OF CONTENTS

LIST OF TABLES	viii
LIST OF FIGURES	ix
I. INTRODUCTION	1
II. BACKGROUND	4
a. Boundary structure	4
b. Supercell-boundary interaction	5
c. Quantifying distances	7
III. METHODS	10
a. Data sources	10
b. IDV analysis	13
c. Temperature gradient analysis	15
d. Statistical methods	16
IV. RESULTS	18
a. Climatological information	18
b. Angle of interaction	19
c. Temperature gradient distribution	21
d. Boundary distance distribution	23
V. DISCUSSION	33
VI. CONCLUSION	37
BIBLIOGRAPHY	40

LIST OF TABLES

TABLE 1: 25 May 2016 case distances with tornado reports 43

TABLE 2: 9 April 2011 case distances with tornado reports 44

TABLE 3: Average error in analyzed distances 44

TABLE 4: Total number of reports in distance distributions 44

TABLE 5: Total number of reports in temperature gradient distributions 45

TABLE 6: Temperature gradient distribution statistics 45

TABLE 7: Temperature gradient 2-Way KS-Test results 46

TABLE 8: Distance distribution statistics 46

TABLE 9: Statistics for significantly severe reports 47

TABLE 10: Total number of significantly severe reports 47

TABLE 11: Majority distances for normal distributions 47

TABLE 12: Majority distances for non-normal distributions 47

TABLE 13: Distance 2-Way KS-Test results 48

LIST OF FIGURES

FIGURE 1: Surface analyses from the 25 May 2016 case 49

FIGURE 2: Boundary distance analysis for 25 May 2016 case 50

FIGURE 3: Boundary cross-section from Maddox et al. (1980) 51

FIGURE 4: Baroclinic horizontal vorticity figure from Markowski et al. (1998a) 51

FIGURE 5: Storm track figure from Rasmussen et al. (2000) 52

FIGURE 6: Cumulative distribution function example 52

FIGURE 7: Total number of cases per year 53

FIGURE 8: Total number of cases per month 53

FIGURE 9: Total number of cases per 20-minutes 54

FIGURE 10: Supercell-boundary interaction angles 55

FIGURE 11: Average temperature gradient per boundary type 55

FIGURE 12: Temperature gradient distributions 56

FIGURE 13: Average distance per boundary type 57

FIGURE 14: Average distance in lifetime stages per boundary type 58

FIGURE 15: Supercell motion vectors with severe reports 59-60

FIGURE 16: Distance and significantly severe report distributions 61

FIGURE 17: Distances containing the majority of severe reports 62

I. INTRODUCTION

Several studies have indicated that storms are more likely to become supercells and produce severe weather near a surface boundary (e.g., Maddox et al. 1980; Markowski et al. 1998b; Rasmussen et al. 2000; Bunkers et al. 2006b). This relationship bears out in the observations, as illustrated by the event on 25 May 2016. The 1300 UTC Day 1 Outlook issued by the Storm Prediction Center (SPC) indicated a marginal risk area over the eastern half of the Great Plains, citing that there will be "little forcing for ascent" in the region. Subsequent updates to the Day 1 Outlook at 1630 and 2000 UTC both acknowledge the incredibly unstable air mass over eastern Kansas, yet only indicate the possibility for an isolated, brief tornado. At 2000 UTC, the atmosphere was ripe for strong, rotating storms, based on observed convective available potential energy (CAPE) values exceeding 2000 J/kg and 0-3 km storm-relative helicity values of at least 100 m^2/s^2 in most of Kansas and over 200 m^2/s^2 in southeastern Kansas.

Earlier that day, convection produced an outflow boundary over northeastern Kansas (Fig. 1a). Over the next several hours, the outflow boundary moved southward, eventually retreating back northward as a warm front (Fig. 1b, c). An isolated storm initiated at 2200 UTC in the vicinity of the warm front analyzed at 2100 UTC by the Weather Prediction Center (WPC; cf. Figs. 1c and 2a) and rapidly developed into a supercell. At 2308 UTC, when the isolated supercell was south of Minneapolis, KS, it produced its first tornado - an EF0 with a 0.47-mile path length. This supercell continued to produce 4 separate tornadoes, including an EF4 tornado with a 26-mile path length which was on the ground for 90 minutes (Fig. 2; Table 1). As indicated in Table 1, the supercell initially became tornadic at 20.99 km from the warm front in the cool sector.

The EF4 Chapman, Kansas tornado developed 1.94 km in the cool sector as the warm front began stalling out to become a stationary front across central Kansas. Of the 8 remaining tornado reports, 6 occurred within 10 km of the cool side of the surface boundary. The proximity of this isolated supercell to the boundary is a likely reason why violent tornadoes formed that day.

This event illustrates some consistencies with previous studies on supercell-boundary interaction. Markowski et al. (1998a) demonstrated that tornadoes in the original Verification of the Origins of Rotation in Tornadoes Experiment (VORTEX; Rasmussen et al. 1994) tended to occur near boundaries; specifically, within 30 km on the cool side and 10 km on the warm side. In the 25 May 2016 case, all of the significant (EF2 or higher) tornado reports occurred close to the boundary, within this specified range. Interestingly, the supercell first became tornadic farther away from the boundary, at more than 20 km into the cool sector (Table 1). This indicates that the conclusions outlined by Markowski et al. (1998a) provide a valid region surrounding the boundary in which tornadoes form. However, other studies have shown that there is not a clearly defined range on either side of the boundary in which severe weather is likely. For example, Fierro et al. (2006) found that supercells were able to remain tornadic within 40 km of a boundary, which also encapsulates all reports within the 25 May 2016 case study, but indicates inconsistency in the literature with regard to where severe weather is most likely near a boundary.

While the 25 May 2016 case study complied with the limits described in Markowski et al. (1998a) for tornadoes, there are also examples of severe weather occurring at a distance that does not align well with neither the Markowski et al. (1998a)

nor the Fierro et al. (2006) conclusions. This is illustrated by a case on 9 April 2011, where a warm front passed over Central Iowa around 2300 UTC, bringing with it dew points over 70°F, CAPE over 4000 J/kg, 0-6 km wind shear of 60 knots, and 0-1 km storm-relative helicity values over 400 m^2/s^2. At 2300 UTC, an isolated supercell formed just on the warm side of the boundary, with distances reported in Table 2 throughout the supercell's lifetime. The supercell quickly produced 1.75" hail at 2317 UTC and became tornadic at 2320 UTC with an EF3 tornado, a mere 10.77 km in the warm sector from the boundary. While the initial time of tornadogenesis nearly aligns with the distances in Markowski et al. (1998a), the supercell remains tornadic (and at times significantly tornadic) until 0318 UTC when it is over 60 km in the warm sector, much farther from the boundary than outlined in both Markowski et al. (1998a) and Fierro et al. (2006). Severe hail, at times up to 2.00" in diameter, was also continuously produced up to 68 km away from the boundary in the warm sector, begging the question as to whether or not the presence of the warm front nearby played a role; such a connection between boundary proximity and enhancement of other types of severe weather is currently unknown.

Given that not all tornadic supercells interacting with boundaries fit within pre-defined distance ranges from a boundary, additional work is needed to better understand the interactions between supercells and surface boundaries. Particularly, a larger dataset is needed to determine the validity of the original range suggested by Markowski et al. (1998a); it would also be useful to identify whether similar ranges are evident for other severe weather, including large hail and strong winds. Thus, the goal of this study to gain a better understanding of the nature of supercell interaction through quantifying the

relationship between severe reports and nearby surface boundaries; it is anticipated that this knowledge will promote more timely and accurate watches and warnings.

II. BACKGROUND

a) Boundary structure

Several studies have examined the interaction of supercells with boundaries through case studies (Maddox et al. 1980; Markowski et al. 1998a; Rasmussen et al. 2000; Bunkers et al. 2006a; Bunkers et al. 2006b; Garner 2012) and numerical model simulations (Atkins et al. 1999; Houston and Wilhelmson 2012; Laflin and Houston 2012; Gagne II et al. 2012). The first to postulate the physical processes behind storm enhancement via boundary interactions, Maddox et al. (1980) studied four supercells interacting with baroclinic zones. As shown in Fig. 3, these boundaries were characterized by a strong temperature gradient, which acts to modify the wind profile on either side of the boundary, creating horizontal variations in vertical wind shear. On the cool side of boundaries (point C in Fig. 3), winds veer slowly through the sub-cloud layer with height, while winds veer rapidly with height in the hot, moist air mass (point B). These variations in sub-cloud winds act to maximize meso-β moisture convergence and cyclonic vorticity, referred to as the mesoscale intensification effect, which can enhance the development of tornadoes even in less than favorable synoptic conditions by generating more vertical vorticity (Maddox et al. 1980).

Wind profile changes near boundaries not only tend to increase the amount of vertical vorticity present, but can also alter the amount of environmental helicity, key to the development of mid-level rotation (Markowski and Richardson 2010). Notably, helicity can vary drastically over relatively short time and distance scales; variations on the order of 2 magnitudes can occur in less than 100 km or fewer than 3 hours (Markowski et al. 1998b). Such large variations are problematic when forecasting severe

weather, especially tornadoes; it is well-known that baroclinically-generated horizontal vorticity (i.e., produced by mesoscale boundaries) correlates to larger values of storm-relative helicity (SRH), which increases the likelihood of significant (F/EF2 or greater) tornadoes (Rasmussen et al. 2000).

b) Supercell-boundary interaction

Consistent with Maddox (1980)'s mesoscale intensification effect, Markowski et al. (1998a) found that the majority (70%) of the tornadoes studied during the original Verification of the Origins of Rotation in Tornadoes Experiment (VORTEX; Rasmussen et al. 1994) occurred near boundaries. This finding was explained using a conceptual model, wherein the ambient environmental horizontal vorticity is enhanced on the cooler side of the boundary; when a supercell travels near or along the boundary, this vorticity can then be vertically tilted and ingested by the supercell, leading to development or enhancement of the low-level mesocyclone (Fig. 4). Indeed, this has been confirmed by subsequent studies of tornadic supercells traveling along or just into the cool sector of a boundary (e.g., Rasmussen et al. 2000; Gilmore and Wicker 2002; Fierro et al. 2006). After supercells crossed an outflow boundary on 2 June 1995, Rasmussen et al. (2000) observed that, despite large CAPE and SRH throughout the region, only supercells that directly interacted with the outflow boundary became tornadic (Fig. 5). The presence of necessary ingredients for severe weather production near boundaries has been concluded in many studies. In their study on the influence of local environment on lightning in supercells, Gilmore and Wicker (2002) found that low-level shear, CAPE, and moisture were enhanced on the cool side of the boundary. Fierro et al. (2006) also observed

enhancement of vertical velocity, reflectivity, and low-level rotation in those supercells which crossed the boundary into the cool sector.

An additional factor in supercell-boundary interaction is the angle of storm motion relative to the boundary. Both observational studies (Rasmussen et al. 2000; Bunkers et al. 2006b) and numerical simulations (Atkins et al. 1999; Laflin and Houston, 2012) concluded that supercells moving parallel to boundaries contained more intense and longer-lasting mesocyclones. This is because the more time a supercell spends near a boundary, the more it can benefit from the enhanced horizontal and vertical vorticity, wind shear, helicity, and moisture, thus allowing a longer lifetime (Bunkers et al. 2006b). The numerical modeling study of the 16 May 1995 supercell from Atkins et al. (1999) found that when the right mover from the splitting supercell quickly crossed the boundary rather than travelling along the boundary, it had a weaker vorticity which took longer to develop, as well as weaker updrafts.

Studies have also examined whether the temperature gradient influenced supercell intensity, since a stronger temperature gradient leads to more baroclinically-generated vorticity. Atkins et al. (1999) tested this in a series of idealized simulations. When a supercell was placed near a boundary with horizontal wind shear and no temperature gradient, it produced much weaker mesocyclones than when placed near a boundary with both wind shear and a temperature gradient. However, when a supercell was located near boundaries of varying gradient strength (1 to 5 K), there was little difference in the strength or evolution of the low-level mesocyclone. This suggests that only the presence

of a temperature gradient (i.e., some baroclinic vorticity) is needed to produce a stronger mesocyclone.

Weiss et al. (2015) reached a similar conclusion after studying two cases of supercells interacting with baroclinic boundaries. The case with a strong temperature gradient (and thus large baroclinically-generated horizontal vorticity) had a supercell with weakly tornadic and non-tornadic phases, while another case with a weak temperature gradient was associated with a strongly-tornadic storm. The distinguishing feature here was the varying motion of the supercell with respect to the boundary. The weakly/non-tornadic storm was oriented perpendicular to the boundary, while the strongly tornadic storm moved parallel to the boundary. Whether this result that supercell movement with respect to the boundary is more important than the strength of the boundary itself would hold up to a larger set of cases is unknown, and needs to be verified.

c) Quantifying distances

Previous studies have quantified how close a supercell should be to a boundary in order to be considered influenced by its presence. These range from 10 km (proximity promoting tornadogenesis; Markowski et al. 1998a) to 35-40 km (enhancement of low-level mesocyclones; Gilmore and Wicker 2002, Fierro et al. 2006, respectively) to 60 km (Rasmussen et al. 2000) to 200 km (Gagne II et al. 2012). While 200 km is arguably too far for supercells to be enhanced by a boundary, the range of 60 km on either side of the boundary, as seen in Rasmussen et al. (2000) as the maximum distance from the boundary at which supercells maintained their enhanced low-level rotation, is a more

reasonable distance for supercells to experience enhancement by the boundary dynamics. However, this will need to be verified using a large dataset of observations.

Markowski et al. (1998a) was the first to suggest a specific range of influence (10 km on the warm side to 30 km on the cool side of a boundary) leading to enhanced severe weather production based on observations. Other studies, such as Boustead et al. (2013), have relied on this range to categorize boundary vs. non-boundary cases. However, it is unclear whether the 40 km wide range identified by Markowski et al. (1998a) can be generalized to all supercells. For example, the 9 April 2011 case described in the introduction suggests boundary enhancement at a greater distance. Additional study is needed to determine the true scope of influence that boundaries have on the development of supercellular tornadoes, as well as other forms of severe weather including hail and wind, as well as whether boundary strength plays a role in severe weather enhancement. A well-defined range based on a large number of observations would provide more concrete information that forecasters can rely on to identify where tornadoes and other severe weather are most likely to form.

In summary, enhanced vorticity and moisture convergence, owing to the differing wind profiles on either side of a boundary, work to intensify supercells and make them more likely to produce tornadoes (Maddox et al. 1980). The environmental baroclinically-generated horizontal vorticity can be vertically tilted, which, in conjunction with the increased amount of SRH present at surface boundaries, may lead to tornadogenesis the longer the supercell is in the proximity of the boundary (Markowski et al. 1998b). However, what constitutes as the “proximity” of the boundary has only been

defined in Markowski et al. (1998a) for tornadoes, and it is unclear the extent to which this is consistent with observations, as well as whether the range can be applied to other severe weather types. Additionally, while it appears that boundary strength is not a distinguishing factor (Atkins et al. 1999; Weiss et al. 2015), it is unknown whether boundary type plays a role. This study will investigate how close a supercell needs to be to a boundary in order to see the production of severe weather (winds, hail, tornadoes) or the enhancement of severe weather, as well as how this may relate to boundary type and strength to assist forecasters in predicting which supercells are more likely to produce severe weather.

III. METHODS

To address the goals of this study, a large number of isolated supercells located near boundaries were identified and then tracked throughout their lifetime, along with their associated severe reports (hail, wind, and tornadoes). This time-lapse approach was used to help quantify the distance at which supercells are influenced by boundaries.

In this study, the interaction of supercells with boundaries will be limited to outflow boundaries, stationary fronts, and warm fronts. Outflow boundaries are a mesoscale feature that result from the cold pool of a storm rushing radially outward into the warmer environmental air (Markowski and Richardson 2010). Stationary fronts are characterized by two contiguous different air masses with neither progressing into the other. Conversely, warm fronts depict a warmer air mass moving into a region with cooler environmental air (Lackmann 2012). Drylines are excluded for the nature of supercells to develop along them and then steer away, and cold fronts often progress over supercells too quickly, inhibiting any prolonged interaction to take place and be studied.

To aid in statistical analysis, a goal of identifying thirty supercell cases for each boundary type was made. Cases were selected between the months of March and June, when supercells are most frequent, and in the Great Plains away from the complicating effects of terrain. Between 2005 and 2016, 38 outflow boundary cases, 46 stationary front cases, and 36 warm front cases were identified.

a) Data sources

Cases were chosen from the Severe Weather Event Archive (SWEA) from the SPC (SPC Severe Weather Events Archive). The primary concern with using SPC storm

reports as proxies for severe weather occurring within a storm is the population bias; essentially, if one area is not as densely populated as another, it is not as likely that severe weather occurring in that area will be reported to the National Weather Service (NWS). Additionally, for all cases in the SWEA prior to the year 2012, the filtered storm reports are not available. Filtered storm reports were used for cases after 2012; for cases prior to 2012, reports were filtered by hand. If there were reports from the same time, with locations within 0.01 coordinate degree of one another, and were the same quantity (e.g., same hail size or wind speed), then this group of reports was "filtered" down into a single representative report. Additionally, Edwards (2016) illustrated how human reporting of severe wind reports is often incorrect due to the difference between perceived wind speed and actual wind speed, as well as the basis for wind reports in SPC to be based on fallen tree limbs rather than quantifiable data. Thus, any trends regarding wind reports may be less robust. Given these difficulties with SPC storm reports, a possible alternative would be to use radar interpolated values for hail size, wind speeds, and tornado detection via the presence of a tornado vortex signature (TVS). However, these values are not always verified by reports on the ground, and are computed by utilizing only vertically integrated liquid (VIL), maximum reflectivity, and temperature profile (Severe Hail Index). Although the population bias from the SPC storm reports affects the results of this study, it served as the best data source to identify storm enhancement as quantified by the number and intensity of severe weather reports.

Once a severe weather day was found in the SWEA, the WPC surface analysis archive was used to investigate whether one of the desired boundaries was present. The surface analysis primarily helped to locate stationary and warm fronts, as well as more

prominent outflow boundaries. For smaller, more mesoscale outflow boundaries, the National Centers for Environmental Information (NCEI) Radar Data page, which shows archived radar composites in 5-minute intervals, was used to see if an outflow boundary was resolved by a radar.

Following selection of a case based on proximity to a boundary and production of severe weather, individual storms were further examined to verify they were supercells. This was achieved using archived Level 3 radar data visualized in the NOAA Weather and Climate Toolkit. If the Mesocyclone Detection Algorithm (MDA) icon was present, then the storm was confirmed as a supercell. Alternatively, if the storm in question produced a tornado, then it was assumed to be a supercell and this process was not conducted. This examination reduced the total number of cases to 108, composing of 35 outflow cases, 41 stationary cases, and 32 warm front cases.

For individual storm analysis and tracking, Level 2 radar data from the NCEI Radar Archives was downloaded for the lifetime of the supercell, as opposed to Level 3 data so that lower level rotation could be detected. However, Level 2 data was not available for all storms; four outflow cases, one stationary case, and three warm cases were thrown out because there was no Level 2 radar data available; therefore, a total of 31 outflow cases, 40 stationary cases, and 30 warm front cases remained.

The surface data used to verify the presence of a boundary and determine its intensity was Surface Airways Observations (SAO) data, downloaded from the Iowa State Environmental Mesonet (IEM) webpage. SAO data is a combination of ASOS stations and extra airport stations, and are maintained by the National Weather Service,

US Air Force Air Weather Service, US Navy, and the US Federal Aviation Administration (U.S. Global Surface Airways Hourly Observations, NCEI Climate Database Modernization Program). This surface data was overlaid on the radar imagery so that boundary locations could be more precisely identified. Specific boundary locations were lined up with the WPC analyses, and then interpolated between the 3-hourly analyses available based on the surface data present. As the surface stations updated every twenty minutes, a new distance analysis was conducted at this time interval. The availability of ASOS archives further restricted the number of cases to 30 outflow boundary cases, 35 stationary front cases, and 30 warm front cases; for the purposes of this study, 30 cases per boundary type were analyzed for as much consistency as possible in analyzed severe reports for each boundary type. Because the stationary boundary still had greater than the 30 desired cases available, each case was assigned a number from 1 to the total number of cases. A random number generator then decided which cases would be analyzed, bringing the final total to 90 cases with 30 per boundary. Note that if more than one supercell was present near the boundary of interest, each supercell was counted as its own individual case.

b) IDV analysis

Utilizing the drawing tool in the Integrated Data Viewer (IDV), a straight line was drawn from the tip of the hook echo, and if no hook echo was present, then the distance was measured from the storm centroid to the boundary. The majority of all cases did have a hook echo present, including approximately two-thirds (66.67%) of all outflow boundary cases, 83.33% of all stationary boundary cases, and 76.67% of all warm front

cases. In the drawing tool window, the length of the line in kilometers is displayed and then recorded by the researcher. This measurement is repeated every 20 minutes and occurs from the time the supercell formed until its dissipation or transition into a mesoscale convective system (MCS). The end result of this methodology is an animation of the supercell(s) producing severe weather and the surface boundary. Once the surface observations, radar imagery, analyzed front, and measurement line connecting the supercell to the boundary are present, the image is recorded to make a loop tracking the supercell's position relative to the boundary. An example of this process using a case from 9-10 April 2011 with the quantitative distances from the boundary is shown in Table 2.

To correlate individual (filtered) severe weather reports with their corresponding supercell, the recorded coordinates of the severe report were compared to the placement of the supercell using a radar image from the same time as the report. If the severe report location aligned with the supercell location, the time and size (hail), speed (wind), or EF scale (tornado, via the Storm Event Database) was recorded. In order to determine the distance at which the report occurred, the recorded time in the SPC SWEA is linearly interpolated from the 20-minute interval recorded distances. For example, if a report occurred at 2014 UTC, the distances recorded at 2000 and 2020 UTC are linearly interpolated to find the distance of the supercell at 2014 UTC.

One limitation of this study is that the surface analyses and measured distances for each of the supercells may be subject to error. When using IDV to measure the distance between a supercell and boundary, a few pixels off may result in an error as

large as 10 km, which would alter the interpolated distances of the severe reports. Additionally, the analyzed location of the surface boundaries between WPC analyses was largely dependent on the density of surface weather stations. If there were sparse reports at the time of analysis, the location of the boundary may also be off by several kilometers. To quantify the amount of subjectivity present in this study, a second analysis was conducted by a third-party researcher on one randomly chosen case per boundary type. The average difference in analyzed distances per boundary type is detailed in Table 3, with the average error being 10.92 km. This qualification on the distances concluded from this study align with the +/- 10 km error stated in Markowski et al. (1998a); thus, a label of +/- 10 km of each report will be included in the final figure of this study.

c) Temperature gradient analysis

To assess the influence of boundary strength on severe weather production, the temperature gradient at the time of severe weather reports was also collected. National Weather Service (NWS) Automated Surface Observational System (ASOS) and Remote Automated Weather Stations (RAWS) observations were utilized to determine the temperature difference across the boundary, well into the warm and cool sectors rather than the two stations immediately closest to the boundary. The two sites closest to the boundary were chosen so the full strength of the boundary is determined, and then the distance between the two stations was measured every twenty minutes. The average distance between two observations sites was 190.3 km with an average temperature gradient of 0.064 ºC/km. Sanders (1999) stated that a temperature gradient of 8ºC over 110 km, or 0.073 ºC/km, was considered strong and a gradient of 8ºC over 220 km, or

0.036 ºC/km, as moderate. Therefore, the gradients analyzed in this study are classified more as strong than moderate. Using the same technique as above, the time of the storm report was then linearly interpolated between the two values of temperature gradient, and then that value was classified to the specific boundary and severe weather type associated with the severe weather report.

d) Statistical methods

The collection of distances of storm reports resulted in 9 separate distributions: tornado reports generated near outflow boundaries, warm fronts, or stationary fronts; hail reports generated near outflow boundaries, warm fronts, or stationary fronts; and wind reports generated near outflow boundaries, warm fronts, or stationary fronts. To assess the normality of these distributions, the Kolmogorov-Smirnov test (KS-test) was utilized so that one standard deviation on either side of a distribution's mean could be used to signify where the bulk of the data is located. The KS-test is a statistical test which determines normality by comparing the empirical cumulative distribution function (ECDF) of the tested distribution versus the cumulative distribution function (CDF) of a reference normal distribution with a specified mean and standard deviation. The probability of a random element from the dataset having a value less than the one on the x-axis is plotted on the y-axis. This results in an S-shaped curve with the final point being (x_{max},1) because the largest value from the dataset has a 100 percent probability that a random element from the dataset would be less than that largest value (e.g., Fig. 6). The null hypothesis of the KS-test, H_o, is that the tested distribution is normal when compared to the specified mean and standard deviation. If the p-value of this test is less than 0.05,

then H_o is rejected in favor of the alternative hypothesis, H_1, which is that the distribution is not normal. In order for this test to be effective, at least 30 elements are required for each distribution.

There is also a Two-Way KS-test, comparing two test distributions instead of a test distribution to a specified normal distribution. H_o for the Two-Way KS-test is that both test distributions come from the same population distribution, while H_1 is that both distributions cannot be subsets of the same population. Similar to the One-Way KS-test, at least 30 elements are required per distribution tested. However, the wind reports for both the warm and outflow boundary distributions do not total more than 30, so they are unable to be statistically tested at this time (Table 4). For the purposes of this research, both tests will be used to compare the distance at which severe reports are received per boundary.

IV. RESULTS

a) Climatological information

Each of the 90 cases included in this study occurred between 2005 and 2016 during the spring months (March, April, May, and June) to encompass the climatological peak in severe weather. The annual distribution of all cases varies year to year, but there is no consistent relationship of note (Fig. 7). The monthly distribution of cases shows that most occur in May and June, as expected (Fig. 8). There is a large difference in monthly distribution with March only containing one outflow boundary case and June containing 7 outflow boundary cases, 22 stationary front cases, and 12 warm front cases. The outflow boundary cases are the only ones to not have their peak in June; instead, their peak is in May with 13 cases out of the 30 total.

In terms of the time of day at which these cases were active, more notable patterns were evident. The frequency of occurrence based on 20-minute intervals is shown in Fig. 9. Both stationary and warm front cases are most frequent between 2200 and 0100 UTC, in stark contrast to outflow boundary supercells, which have a maximum in occurrence at 0400 UTC. This delay is likely because outflow boundary cases rely on prior convection to develop an outflow boundary and develop supercells in its proximity for interaction, as opposed to warm or stationary fronts which often have convection initiate on the boundary or along an associated dryline. Notably, the later occurrence of outflow boundary-supercell interactions indicates that nocturnal cooling likely had a greater effect on the evolution of these storms (including their production of severe weather), less so than the warm front and stationary front cases. Therefore, it is worth nothing that outflow

cases have fewer overall severe reports compared to stationary or warm front cases (Table 4).

b) Angle of interaction

The degree of interaction of a supercell with a nearby boundary is limited by the angle of supercell motion relative to the boundary (Atkins et al. 1999; Rasmussen et al. 2000; Bunkers et al. 2006b; Laflin and Houston 2012). For each case, the average angle at which the supercell travels throughout its lifetime with respect to the boundary is analyzed. For supercells interacting with outflow boundaries, they interact at either small (10-45º) angles (i.e., more parallel to the boundary), or at large (60-90º) angles (i.e., more perpendicular; Fig. 10a). The predominant supercell-outflow boundary angle is 90º, which is likely due to the dominant flow of the outflow boundary steering the supercell when the interaction takes place. The secondary angle mode is 30º, which would encapsulate the supercells crossing the boundary over a longer period of time at a shallower angle. Of the 114 tornado reports associated with outflow-interacting supercells, 58% of the tornado reports occurred in those supercells crossing at small angles (10 to 45º), while 42% of tornado reports were associated with supercells that crossed at larger angles (60 to 90º), consistent with previous studies noting the importance of the supercell's motion relative to the boundary with regards to tornado production (e.g., Bunkers et al. 2006b; Weiss et al. 2015). Out of the 48 total significant tornado reports (>F/EF2) associated with outflow boundaries, 18 of them occurred with supercell-boundary angles less than 45º and the remaining 30 significant tornado reports occurred with angles greater than 45º. However, the 30 significant reports are skewed by a single outlier case that crossed at a large angle. Focusing on just the supercell cases, 12

produced significant tornadoes; only 3 of these interacted with the outflow boundary at an angle greater than 45º. Therefore, although there were more *total* significant tornadoes associated with larger supercell-boundary angles, there were more *cases* which produced significant tornadoes in smaller supercell-boundary angles, still confirming the importance of supercell motion relative to the boundary when assessing the potential for tornado production.

In supercell-stationary front interactions, Fig. 10b also shows a dichotomous distribution; one cluster is located from 0 to 45º, and another from 60 to 80º. Similar to the outflow boundary cases, of the 88 total tornado reports, 55.6% of them occurred in the 0 to 45º range, and the remaining 44.4% occurred in the 60 to 80º range, also confirming the conclusion that the smaller the angle of interaction, the stronger the low-level rotation and potential for tornadogenesis. Additionally, out of the 11 total significant tornado reports that occurred in stationary boundary cases, 10 of the 11 occurred in storms that interacted with supercells at an angle less than 45°, while only one case was from a supercell interacting with the boundary at a large angle. Therefore, more total tornado reports occurred with small supercell-boundary angles, as well as nearly all of the significantly severe tornado reports.

A bimodal distribution was also evident in warm front cases, between 10 to 45º and 70 to 90º (Fig. 10c). The 172 total tornado reports were split evenly between the two modes; even so, significantly severe tornado reports revealed a similar pattern as in the outflow and stationary boundaries, wherein the majority of significantly severe reports

(32 of 41) occurred with small supercell-boundary interaction angles while a minority (9) occurred with larger interaction angles.

The angle at which the supercell crosses or interacts with the boundary has been shown to greatly influence its proclivity to produce tornadoes (Bunkers et al. 2006b, Weiss et al. 2015). This study also confirmed that when supercells cross boundaries at smaller angles (less than 45º), not only is that supercell more likely to produce a tornado than if it were to cross at a large angle (greater than 45º), but it is also more likely to produce a significantly severe tornado when crossing at smaller angles.

c) Temperature gradient distributions

An additional point of focus in this study is the role that temperature gradient strength plays in severe weather production. Overall, the distributions of the average temperature gradient in each case have fairly similar medians and interquartile ranges (Fig. 11). Interestingly, the average temperature gradients observed in warm front cases have far more outliers containing stronger temperature gradients. Due to the overall similarity in average temperature gradient strength per boundary type, each boundary average will be broken up by severe reports to see if the temperature gradient could assist in forecasting different severe weather types.

Figure 12 shows the distributions of temperature gradient at the time of severe report generation for each boundary type for all three severe report types. However, due to the limited number of wind reports within each case and time limitations, only tornado and hail distributions for each of the three boundary types had sufficient data points for statistical analysis (Table 5). Interestingly, tornadoes tended to occur more frequently

when the temperature gradient was *stronger*, with comparatively weaker temperature gradients were associated with hail and wind reports (Fig. 12; Table 6). The general trend presented here of tornadoes associated with stronger temperature gradients than hail or wind reports suggests that the stronger baroclinically generated horizontal vorticity would help contribute to more streamwise vorticity ingested in the supercell, thus increasing low-level rotation and the proclivity for tornadogenesis (e.g., Rasmussen et al. 2000; Bunkers et al. 2006b). Indeed, this larger gradient for tornadoes is statistically significant compared to hail reports in both stationary and warm fronts (Table 7). While this is not the case within outflow boundaries, the difference is close to significant.

While tornadoes tend to occur when stronger temperature gradients are present, the magnitude of the gradient for all boundary types is not necessarily similar. Table 7 illustrates that comparisons of temperature gradient distributions among tornadoes associated with different boundaries were significantly different for outflow vs. stationary and warm vs. stationary. Similarly, the temperature gradients associated with hail reports for different boundaries are statistically different for outflow vs. stationary and warm vs. stationary. For both tornado and hail reports, those occurring near warm fronts were associated with the strongest median temperature gradient, followed by outflow boundary temperature gradient, and then the stationary front median temperature gradient being the weakest. The temperature gradient of the surface boundaries may be influenced by the nocturnal transition, which cools the environmental air, therefore reducing the temperature gradient. This change in temperature gradient is most predominant in outflow boundaries, as their average time of occurrence is 4 hours later than warm and stationary fronts, thus causing them to be more susceptible to environmental temperature

decreases after the nocturnal transition. Distributions of tornado and hail reports for stationary fronts also show far more reports less than 0.03°C/km, which would result in a lower median. Overall, the different distributions for both tornado and hail reports implies that the type of boundary can be used to distinguish between tornado and hail formation for stationary and warm fronts by using different temperature gradient thresholds, as both tornadoes and hail are produced in a variety of temperature gradients, which are generally sensitive to the boundary type.

d) Boundary distance distributions

One of the primary goals of this study was to investigate how the distance of a supercell from a boundary affects severe weather production. For all three types of boundaries, the average distance of a supercell to the boundary it is interacting with lies in the warm sector (16.81 km away; Fig. 13). Supercells near outflow boundaries have the greatest median distance of 41.68 km (Fig. 13a), while stationary cases are 8.73 km away (Fig. 13b), and warm front cases lie only 0.76 km into the warm sector (Fig. 13c). This result is fairly unsurprising, as supercells tend to spend a majority of their time on the warm side of a boundary due to the availability of warm, moist air and sufficient CAPE.

While supercells tend to be located on the warm side of a boundary, there is variation over time. The average boundary distance at the initial development, midpoint, and demise or upscaling of each supercell's lifetime shows clear trends. For all boundary types, supercells on average move progressively towards and into the cool side of the boundary over time (Fig. 14). Note that this does not necessarily mean that all of these supercells moved towards the cool sector; for example, in some cases, the outflow

boundary was moving faster towards the supercell, resulting in a decreasing net distance from the cool side of the boundary. Even so, supercells approaching or being located within the cool sector near the end of their lifetime makes physical sense, as these areas tend to be associated with stronger convective inhibition and weaker instability, leading to storm weakening or demise.

Given the presence of enhanced baroclinicity, vorticity, wind shear, and convergence associated with surface boundaries (e.g., Maddox et al. 1980; Markowski et al. 1998b; Atkins et al. 1999; Bunkers et al. 2006b), it is expected that there will be a relationship between supercell movement and the generation of severe weather. By plotting the overall direction of motion (as either towards or away from the boundary) for each supercell, it is evident that the frequency of storm report occurrences increases the closer the supercell travels toward the boundary (Fig. 15). Overall, 27 out of the 90 total cases travel from the cool sector toward the warm sector, meaning that 63 of the total 90 cases travel toward the cool sector, which is consistent with the average storm motion derived from Fig. 14. Qualitatively, tornado reports tend to increase just before or after crossing the boundary, implying that the interaction of the supercell with the boundary is what led to tornadogenesis. Hail reports also tend to increase in frequency the closer the supercell moves to the boundary, meaning the enhanced vorticity, energy, and moisture leads to a stronger updraft and thus more formation of hail. These features are also evident when focusing on a narrower range (within 60 km of either side of the boundary, Fig. 15 d-f; Rasmussen et al. 2000). While a few cases from each boundary type are omitted by utilizing this narrower range, actual boundary enhancement is much more likely.

For outflow boundary cases (Fig. 15a, d), five of the thirty total cases moved from cooler air into warmer air, and twenty-five moved from warmer air toward cooler air behind the boundary. Of the six tornadic cases that crossed the boundary, four of them either maintained their tornadic activity or became tornadic after crossing the boundary. In stationary front cases (Fig. 15b, e), twelve of the thirty cases progressed from cooler air toward warmer air, and eighteen moved from the warmer air toward the cooler air. Of the seven tornadic cells that crossed the boundary, five of them remained tornadic or developed a tornado after crossing. Lastly, for warm front cases, ten of the thirty cases moved toward warmer air and twenty moved toward cooler air (Fig. 15c, f). Of the eleven cases that were tornadic and crossed the boundary, ten of them maintained or developed tornadic activity after crossing. The proclivity for a majority of storms crossing a boundary to maintain or develop tornadic activity (e.g., Rasmussen et al. 2000), as well as how the frequency of reports increases as several supercells approach the boundary, reinforces the idea that a boundary enhances low-level rotation, potentially contributing to tornadogenesis. The specific distances at which tornado production occurred, as well as hail and wind reports, will be elucidated next.

To identify where boundary-induced enhancement of severe weather is located, histograms of each report type binned by the distance at which they occurred are displayed in Fig. 16. Rasmussen et al. (2000) identified 60 km as the maximum distance from the boundary where supercells are likely to experience enhanced low-level rotation due to the presence of the boundary. Given that the width of boundary is on a relatively small horizontal scale (~10 km or less), 60 km is a relatively reasonable cutoff distance. While this threshold was based on a single case study, the majority of the storm reports

used in this research were produced within 60 km of the boundary, lending credence to this choice. Additional thresholds will be assessed in the future to ensure that the results are not sensitive to small variations in this cutoff distance from the boundary.

Table 8 shows the mean, median, mode, and skewness for each report distance distribution for all boundary types. For supercells interacting with outflow boundaries, tornadoes tend to occur further into the warm sector than hail or wind reports, as evidenced by their larger mean and median distance. The distributions of each report type for outflow boundaries all favor the warm sector (positive values), in which the majority of reports occur. However, the peak value of the tornado distribution is closer to the boundary. The skewness of each report distribution within outflow boundaries is negative, implying that the distribution is skewed to the left, so the medians are all higher than the means in the warm sector. This is visually confirmed in Fig. 16a-c, where it is also evident that the modes for each type of severe report types is located between 30-40 km in the warm sector. Given that most of the outflow-interacting supercells were moving *toward* the cooler air behind the boundary, the increased frequency of reports occurring in the 30-40 km range in the warm sector indicate that this is a distance at which supercell enhancement is preferred. This range is consistent with the distances proposed in Gilmore and Wicker (2002) and Fierro et al. (2006) of 35 to 40 km from the outflow boundary when the supercells exhibited stronger low-level rotation, thus enhancing supercell strength and proclivity for tornadogenesis.

The severe report distance distributions for stationary boundaries show that the mean and median for all report types fall on the cool side of the boundary, in contrast to

the outflow boundary observations (Table 8). However, the median lies further in the cool sector than the mean, thus implying the data is right skewed, as verified by the positive skewness values, indicating the bulk of reports fall in the cool sector. The dominant modes for each report type occur at varying distances, all in the cool sector: 30 km, 25 km, and 50 km for hail, tornado, and wind reports, respectively (Fig. 16d-f). Notably, a secondary mode is evident in the hail distribution, near 30 km in the warm sector. This may be due to the split in storm-motion of all cases included; the secondary mode of 30 km in the warm sector may be a result of supercells traveling toward the cool sector and approaching the zone which favors supercell enhancement. All modes also fall in the range of 60 km on the cool side of the boundary, as identified in Rasmussen et al. (2000), which encompasses all the means, medians, and modes of the stationary front distributions. Unlike the commonly-used distances in Markowski et al. (1998a), Rasmussen et al. (2000)'s analyzed distances align more with the average occurrences of *all* severe weather types, as opposed to just tornadoes.

For severe reports in supercells interacting with warm fronts, the most notable feature is how the tornado report distribution heavily favors the warm sector (similar to the outflow-interacting supercells), while the hail and wind reports seem more evenly distributed on either side of the boundary (Fig. 16g-i). Table 8 indicates that for both tornado and hail reports, the median is greater than the mean and the data is skewed to the left, as confirmed by the negative skewness values, while the data is right skewed for wind reports. This agrees with the visual representation that the majority of tornado and hail reports occur in the warm sector, while the majority of wind reports occur in the cool sector. Both tornado and wind reports occurring near warm fronts match the distributions

from stationary and outflow boundary distributions with a mean distance closer to the boundary than the median. However, the hail report distribution has the median in the warm sector and the mean in the cool sector, which implies that there are more extreme distances reported in the cool sector rather than in the warm sector. Indeed, the primary mode for hail reports near warm fronts is 15 km in the warm sector, and the secondary mode is 60 km in the cool sector, which would explain why the mean is further in the cool sector than the median. The mode for tornado reports is 40 km in the warm sector, while wind reports have a mode 40 km in the cool sector, but with only 17 reports total, a distinct distribution pattern is difficult to ascertain. Aside from the secondary mode of extreme values in the hail distribution, all of the means, medians, and modes for all three distribution also falls in the ranges from Gilmore and Wicker (2002) and Fierro et al. (2006) of 35-40 km from the boundary for storms to be enhanced.

On each of the nine distributions in Fig. 16, the darker shaded distribution marks the significantly severe reports (tornadoes > F/EF2, hail > 2.00", wind > 65 mph) for each report and boundary type. For all distributions except stationary-wind and all warm front distributions, the mean distance of the significantly severe report distributions was closer to the boundary than the mean distance of all reports. This aligns with the conclusions of severe previous studies (e.g., Maddox et al. 1980; Markowski et al. 1998a; Rasmussen et al. 2000; Bunkers et al. 2006b; Weiss et al. 2015) that boundaries can help enhance storms to produce significantly severe weather. In general, the shape of each significantly severe distribution matches the parent distribution of all reports within that report-boundary type distribution. One limitation of this study is that the number of significantly severe reports is not enough to make a statistical comparison, nor identify a

clear mode. Additionally, the sample sizes for all wind reports were far smaller than the tornado or hail reports for both outflow and stationary fronts; therefore, more significantly severe storm reports would need to be gathered in order to make a meaningful comparison to the overall severe report distribution.

Table 9 displays the mean and median for significantly severe hail and tornado reports per boundary type. With the exception of outflow boundary cases, significantly severe tornadoes occur at closer distances to the boundary than significant hail, which supports the theory that tornadoes require the stronger velocity, wind shear, and helicity near boundaries. When compared to the means and medians of the overall distance distributions in Table 6, the mean of tornado-outflow significant severe reports is closer to the boundary, as well as both the mean and median of the significantly severe hail reports near outflow boundaries. For stationary boundaries, both the mean and median for tornado and hail distributions are closer to the boundary for significantly severe reports than all reports in general. None of the significantly severe reports near warm fronts have a closer mean or median to the boundary, but Table 10 explains that this could be a result of sampling error without enough samples to justify a comparison to a distribution with more reports.

Several differences were noted among the distributions of severe reports, both among report types and among boundary types. To identify whether these differences hold any significance, the One-Way KS-test was first utilized to assess the normality of each distribution. The Two-Way KS-test then compared different pairs of distributions within the same report or boundary type. However, both the One-Way and Two-Way KS-

tests require at least 30 data points; the wind reports from both outflow and warm front cases only have 29 and 17 reports, respectively (Table 4). Thus, these distributions were removed from any statistical testing. Additionally, Edwards et al. (2016) highlighted the inherent error present in most severe wind reports; therefore, the stationary wind report distribution will also be omitted from testing. The One-Way KS test compared each severe weather report distribution per boundary type to a normal distribution with their own mean and standard deviation. Three of the remaining 6 distributions were confirmed as normal: outflow boundary tornado and hail reports, as well as stationary front tornado reports. Table 11 lists the distances within which 67.5% (one standard deviation) of severe reports were located for the normal distributions, encompassing a majority of all reports in each distribution.

In order to elucidate the distances in which a majority of reports occur for the non-normal distributions (hail-stationary, tornado-warm, and hail-warm), each side of the boundary was tested using the One-Way KS-Test for normality. Similar to the normal distributions, one standard deviation on either side of the mean report distance in both the warm and cool sectors was used to identify a range in which a majority of reports occur. When separated into the warm and cool sectors, all sectored distributions tested as normal. Table 12 shows the mean and +/- one standard deviation ranges for each sector within each boundary. For each of the three remaining distributions, the standard deviations do not extend further into the warm or cool sector than 50 km, which is further than the 40 km analyzed in Fierro et al. (2000). Comparisons of the significant distances within the same boundary and report type in the Discussion section will help identify how distance to the boundary relates to the type of severe weather which occurs.

The Two-Way KS-Test was used to compare distributions of severe reports for different boundary types (e.g., tornado reports generated in outflow versus stationary boundary cases). Additionally, different severe report distributions are compared within the same boundary type to identify whether, for example, tornado reports are more prevalent at a different distance than hail reports. This resulted in several pairs of distribution comparisons (Table 13); note that only tornado and hail report distributions contained sufficient data points for robust statistical testing. Of all possible combinations of distributions within the same boundary, only warm front severe reports tested as statistically significantly different. The distributions of tornado and hail reports were statistically similar in both outflow and stationary cases, which is consistent with the similar means, medians, and modes listed in Table 8. In other words, within a given boundary type, both outflow and stationary boundaries appear to produce tornadoes and hail in similar locations, most frequently near 30 km in the warm sector for outflow boundaries and near 25 km in the cool sector for stationary boundaries.

However, when comparing similar report type distributions among different boundaries, every comparison was found to be statistically significantly different (Table 13). This means that the range at which tornadoes and hail occur near boundaries is significantly different depending on which boundary type the supercell is near. Therefore, the occurrence of tornadoes and hail is maximized in statistically different distances for each of the three boundaries. This implies that these distributions are distinctive; each boundary type has a unique distribution of severe reports generated by an interacting supercell, further underscoring the need for forecasters to be aware of these variations to appropriately nowcast severe watches and warnings.

V. DISCUSSION

The distributions of severe reports for temperature gradient and distance from the boundary largely depend on both the type of report and the type of boundary. Both the One-Way and Two-Way KS-Tests were used to test whether each distribution was normal and whether any pair of distributions may be related by a "parent" distribution, respectively. For temperature gradient distributions, the comparison of different report types within a boundary type showed that tornado and hail production occurs at statistically different magnitudes, except in outflow boundaries (Table 7). Physically, tornadoes require baroclinically-generated streamwise vorticity (e.g., Davies-Jones and Brooks 1993; Markowski et al. 2002; Dahl et al. 2014), which can be augmented by the presence of surface boundaries (e.g., Markowski et al. 1998a). However, hail production is typically not associated with surface boundaries; such features can provide enhanced convergence and may strengthen updrafts (thus encouraging hail production), but largely speaking, forecasting hail is related to environmental parameters such as CAPE and the freezing level height (e.g., Fawbush and Miller 1953). Thus, the observation that tornadoes are associated with stronger temperature gradients than hail appears to be consistent with our current understanding.

The temperature gradient distributions were also statistically compared by boundary to see, for instance, if tornadoes were more likely produced at a different temperature gradient near stationary fronts than near warm fronts. Surprisingly, temperature gradients were significantly different between tornadoes in outflow versus stationary fronts and stationary versus warm fronts. Hail reports were found have

significantly different temperature gradients for the same boundary comparisons: outflow versus stationary fronts and stationary versus warm fronts. The key boundary type here is the stationary front; as Table 6 shows, the temperature gradient mode for stationary front tornadoes is notably cooler than warm fronts or outflow boundaries. However, physically, the distinction between a stationary and warm front in terms of temperature gradient is not very clear, as a warm front may stall out and become a stationary front or a stationary front can begin to move as a warm front. A larger dataset (i.e., encompassing the temperature gradient of each tornado report instead of a subject; cf. Tables 4 and 5) may help to assess whether this result is representative.

The core of this study was to assess the relationship between severe report generation and distance to nearby surface boundaries. When comparing severe weather generation within a given boundary type, the distributions tended to be similar for outflow and stationary boundaries (Table 13); however, the actual distances differed among boundary types. For example, outflow boundaries produce tornadoes and hail most frequently near 30 km in the warm sector (Table 13; Fig. 16a-c). Conversely, stationary boundaries produce severe weather most frequently near 25 km in the cool sector (Table 13; Fig. 16d-f). This may be a function of the different nature of outflow-supercell and stationary front-supercell interactions; nearly all supercells move toward the cool side of outflow boundaries and dissipate quickly once they reach the cool side (Fig. 15a). On the other hand, supercells interacting with stationary fronts are more evenly distributed in terms of moving away or towards the boundary (Fig. 15b), which would account for the clear bimodal distribution of hail (Fig. 16e). The exception to this finding was severe weather associated with warm fronts. Tornadoes and hail were

produced at statistically different distances; tornadoes most frequently occurred farther in the warm sector than hail (Table 13; Fig. 16g-i).

Within the same report type, all the comparisons were found to be statistically significant (Table 13). In other words, where tornadoes and hail tend to occur is sensitive to the boundary type. Therefore, the distances used to discriminate between tornado and hail production for each boundary type should be unique. These comparisons are summarized in Fig. 17, illustrating the ranges in which the majority of tornado and hail reports occurred; non-normal distributions contain the range for both the warm and cold sectors. This figure demonstrates that, on average, the mode distances at which tornado reports occur is closer to the boundary than the mode distances at which hail reports occur for all boundary types, as verified by Table 8. One possible influence on why distance distributions for boundaries were found to be statistically different is due to storm motion. Tying this more to how the supercells interacted with the different boundaries, due to the diverse nature of the cases analyzed per boundary, would help determine why the distributions near different boundaries tested as statistically different. Accounting for supercell motion influencing severe weather production might include whether the supercells were traveling toward the warm or cool sector, as well as the angle at which the supercells moved in relation to the boundary. By taking the direction of storm motion into account (i.e. supercell moving toward the warm or cool sector), the bimodal appearance of some distributions may be reduced as a result of supercells now interacting with the boundary from the same sector of origin, therefore ideally reaching a more universal "critical" distance at which severe weather production occurs. Additionally, distinguishing between large and small angles of interaction would shed

light on whether or not the amount of time a supercell spends near a boundary would influence how much severe weather it produces.

In summation, severe weather occurrence can be best discriminated by a unique temperature gradient for each report type within the same boundary type, and a unique distance for each boundary type. Most significantly severe report distributions indicate that the closer a supercell is to a surface boundary, the more likely it is to ingest the stronger horizontal and vertical vorticity, vertical velocities, moisture, and helicity and then produce significantly severe tornadoes and hail (Rasmussen et al. 2000).

VI. CONCLUSIONS

It has been well-established that surface boundaries can lead to enhanced convection and severe weather. This has primarily been understood in the context of enhancing tornadogenesis due to the increased helicity and baroclinically-generated horizontal vorticity increasing low-level rotation (e.g., Maddox et al. 1980; Markowski et al. 1998a; Atkins et al. 1999), though the extent to which other types of severe weather can be enhanced by the presence of a boundary is less clear. Previous studies have shown supercell enhancement can occur as little as 10 km from the boundary up to 200 km away (e.g., Markowski et al. 1998a; Gagne II et al. 2012). To provide a more conclusive set of distances and to encompass all severe weather types, this study measured the distance at which severe weather occurs for 90 supercells interacting with outflow boundaries, stationary fronts, and warm fronts, with 30 storms for each boundary. Additionally, the influence of temperature gradient strength on severe weather production was studied.

On average, the mode for temperature gradients associated with tornado reports is stronger than the ones required for hail reports. This implies that tornadoes are more dependent on a stronger temperature gradient and thus stronger baroclinically-generated horizontal vorticity while severe hail reports are not as dependent on temperature gradient. The general modes of the distance distributions for tornadoes were closer to the boundary than those for hail or wind reports. Similar to the temperature gradient analysis, this implies that tornado production is more dependent on the horizontal vorticity generated near boundaries as opposed to severe hail or wind reports.

Statistical comparisons using both the One and Two-Way KS-Tests were used to analyze the relationship between boundary and report type on the temperature gradient at which severe weather is produced, as well as the distance of the supercell from the boundary when severe weather is produced. This study concluded that severe weather production near temperature gradients is not as influenced by boundary type, but is more dependent on the type of severe weather. This means that while the temperature gradients for severe weather production may be similar for different boundaries, the temperature gradients that produced severe weather are statistically different when distinguishing the between hail and tornado reports. Conversely, the distances at which severe tornadoes and hail occur were concluded to be statistically different with different boundaries, but not statistically different when compared with different report types. Therefore, for tornado and hail reports in the same boundary, the distances at which severe weather occurs was not found to be significantly different, but the distance at which hail or tornado reports occur has a statistically different distribution for outflow, stationary, and warm fronts. In summation, Fig. 17 demonstrates the distances at which severe weather is most likely to be produced, as differentiated by report and boundary type.

The results of this study are intended to assist forecasters in determining when supercells are most likely to produce severe weather, which can be particularly useful in the midst of an outbreak. To further promote this outcome, future work should seek to extend the number of cases analyzed for both distance and temperature gradient analysis so that all severe weather types can be analyzed and given distances which contain the majority of reports. Additionally, future research should also take storm motion into consideration when generated distributions for the distance at which severe weather is

conducted. For example, making separate distributions for cells which move toward the warm vs. cool sector could help separate the influence of the storm approaching the boundary from the storm moving away from the boundary. Another potential influence of storm motion on this study would be the average angle at which the supercell interacts with the boundary; dividing the distributions by angles less than 45º and greater than 45º could help elucidate different distances for different angles of motion. Once these influences are clarified, future studies should then utilize numerical simulations to determine the physical differences of a supercell interacting with boundaries of different temperature gradients from differing distances.

BIBLIOGRAPHY

Atkins, N. T., Weisman, M. L. and Wicker, L. J. (1999) 'The Influence of Preexisting Boundaries on Supercell Evolution', *Monthly Weather Review*, 127(12), pp. 2910–2927. doi: 10.1175/1520-0493127.

Boustead, J. M., Mayes, B. E., Gargan, W., Leighton, J. L., Phillips, G. and Schumacher, P. N. (2013) 'Discriminating Environmental Conditions for Significant Warm Sector and Boundary Tornadoes in Parts of the Great Plains', *Weather and Forecasting*, 28(6), pp. 1498–1523. doi: 10.1175/waf-d-12-00102.1.

Bunkers, M. J., Hjelmfelt, M. R. and Smith, P. L. (2006) 'An Observational Examination of Long-Lived Supercells. Part I: Characteristics, Evolution, and Demise', *Weather and Forecasting*, 21(5), pp. 673–688. doi: 10.1175/waf949.1.

———, Johnson, J. S., Czepyha, L. J., Grzywacz, J. M., Klimowski, B. A. and Hjelmfelt, M. R. (2006) 'An Observational Examination of Long-Lived Supercells. Part II: Environmental Conditions and Forecasting', *Weather and Forecasting*, 21(5), pp. 689–714. doi: 10.1175/waf952.1.

Dahl, J. M. L., Parker, M. D. and Wicker, L. J. (2014) 'Imported and Storm-Generated Near-Ground Vertical Vorticity in a Simulated Supercell', *Journal of the Atmospheric Sciences*, 71(8), pp. 3027–3051. doi: 10.1175/jas-d-13-0123.1.

Davies-Jones, R. P., and H.E. Brooks, 1993: Mecocyclogenesis from a theoretical persective. The tornado: Its Structure, Dynamics, Prediction, and Hazards, Geophys. Monogr. No. 79, Amer. Geophys. Union, 105-114

Edwards, Roger (2016) 'Estimated Convective Winds: Reliability and Effects on Severe-Storm Climatology', *28th Severe Local Storms Conference*, 14B.6

Fawbush, E. J., and R. C. Miller (1953) 'A method of forecasting hailstone size at the earth's surface', Bull. Amer. Meteor. Soc., 34. 235-244.

Fierro, A. O., Gilmore, M. S., Mansell, E. R., Wicker, L. J. and Straka, J. M. (2006) 'Electrification and Lightning in an Idealized Boundary-Crossing Supercell Simulation of 2 June 1995*', *Monthly Weather Review*, 134(11), pp. 3149–3172. doi: 10.1175/mwr3231.1.

Gagne II, David John, Amy McGovern, Jeffrey B. Basara, Rodger A. Brown. (2012) Tornadic Supercell Environments Analyzed Using Surface and Reanalysis Data: A Spatiotemporal Relational Data-Mining Approach. *Journal of Applied Meteorology and Climatology* **51**:12, 2203-2217.

Houston, A. L. and Wilhelmson, R. B. (2012) 'The Impact of Airmass Boundaries on the Propagation of Deep Convection: A Modeling-Based Study in a High-CAPE, Low-Shear Environment', *Monthly Weather Review*, 140(1), pp. 167–183. doi: 10.1175/mwr-d-10-05033.1.

Lackmann, G. (2012) *Midlatitude Synoptic Meteorology: Dynamics, Analysis, and Forecasting*. Boston, MA: American Meteorological Society.

Maddox, R. A., Hoxit, L. R. and Chappell, C. F. (1980) 'A Study of Tornadic Thunderstorm Interactions with Thermal Boundaries', *Monthly Weather Review*, 108(3), pp. 322–336.doi: 10.1175/1520-0493(1980)108<0322:asotti>2.0.co;2.

Markowski, P. M., Rasmussen, E. N. and Straka, J. M. (1998) 'The Occurrence of Tornadoes in Supercells Interacting with Boundaries during VORTEX-95', *Weather and Forecasting*, 13(3), pp. 852–859. doi: 10.1175/1520-0434(1998)013<0852:tootis>2.0.co;2.

———, Straka, J. M., Rasmussen, E. N. and Blanchard, D. O. (1998) 'Variability of Storm-Relative Helicity during VORTEX', *Monthly Weather Review*, 126(11), pp. 2959–2971. doi: 10.1175/1520-0493(1998)126<2959:vosrhd>2.0.co;2.

———, ———, and ———, (2002) 'Direct surface thermodynamic observations within the rear-flank downdrafts of nontornadic and tornadic supercells. Mon. Wea. Rev., 130 1692-1721

———, and Richardson, Y. P. (2010) *Mesoscale Meteorology in Midlatitudes (Advancing Weather and Climate Science)*. 1st edn. Wiley, John & Sons.

NCDC Climate Database Modernization Program, National Centers for Environmental Information, *NOAA*. <https://www.ncdc.noaa.gov/climate-information/research-programs/climate-database-modernization-program>

Rasmussen, E. N., Richardson, S., Straka, J. M., Markowski, P. M. and Blanchard, D. O. (2000) 'The Association of Significant Tornadoes with a Baroclinic Boundary on 2 June 1995', *Monthly Weather Review*, 128(1), pp. 174–191. doi: 10.1175/1520-0493(2000)128<0174:taostw>2.0.co;2.

———, J. M. Straka, R. Davies-Jones, C. A. Doswell, F. H. Carr, M. D. Eilts, and D. R. Macgorman, 1994: Verification of the Origins of Rotation in Tornadoes Experiment: VORTEX. *Bull. Amer. Meteor. Soc. Bulletin of the American Meteorological Society*, **75**, 995–1006, doi:10.1175/1520-0477(1994)075<0995:votoor>2.0.co;2.

Severe Hail Index (SHI), Mutli-Radar/Multi-Sensor (MRMS) Products Guide, *Warning Decision Training Division, NOAA*. <http://www.wdtb.noaa.gov/courses/MRMS/ProductGuide/SevereWeather/severe-hail-index.php>

SPC Severe Weather Events Archive, Storm Prediction Center, *NOAA's National Weather Service.*

U.S. Global Surface Airways Hourly Observations (DSI-3280), Discover Earth Science Data and Services, *NASA Global Change Master Directory*. <http://gcmd.nasa.gov/records/GCMD_gov.noaa.ncdc.C00215.html>

TABLES

Table 1: Distances over time between the supercell and warm/stationary front on 25 May 2016. Negative distances represent the cool sector.
*Tornado report, **Significant tornado report

Time (UTC)	**Distance (km)**
2200	-29.34
2220	-27.00
2240	-25.44
2300	-21.92*
2320	-19.59
2340	-12.23
0000	-5.84**
0020	-2.27**
0040	-0.96**
0100	-4.49
0120	-13.96**
0140	-12.23
0200	-9.29**
0220	-5.13
0240	-7.28*
0300	-10.72*
0320	-8.32*
0340	-7.75
0400	-7.83

Table 2: Distances over time between the supercell and warm front on 9-10 April 2011. Positive distances represent the warm sector.

*Tornado report, **Significant tornado report

Time (UTC)	**Distance (km)**
2300	18.18
2320	10.77**
2340	19.75
0000	17.50**
0020	20.25**
0040	20.24
0100	25.58
0120	22.39**
0140	24.55**
0200	39.45**
0220	45.82**
0240	61.80*
0300	69.25**
0320	62.01*
0340	61.73
0400	69.25
0420	67.12

Table 3: Average absolute value error in the distances analyzed by the author and a secondary analysis from a third party in randomly selected representative cases per boundary type.

Boundary Type:	**Average Distance Error (km):**
Outflow	5.2
Stationary	9.3
Warm	18.3
Overall	*10.9*

Table 4: Total number of reports per boundary type used in distance distributions.

	Tornado	**Hail**	**Wind**	***Total***
Outflow	71	56	29	*156*
Stationary	51	147	50	*248*
Warm	131	114	17	*262*
Total	*253*	*317*	*96*	*666*

Table 5: Total number of reports per boundary type used in temperature gradient distributions.

	Tornado	**Hail**	**Wind**	***Total***
Outflow	49	32	10	*91*
Stationary	33	36	7	*76*
Warm	34	31	6	*71*
Total	*116*	*99*	*23*	*238*

Table 6: The mean, median, mode, and skewness of all temperature gradient distributions. Mode is listed based on the 0.05°C/km bin used to display the data. Skewness is a measure of the asymmetry of the data around the sample mean. If skewness is negative, the data are spread out more to the left of the mean than to the right. If skewness is positive, the data are spread out more to the right. The skewness of the normal distribution (or any perfectly symmetric distribution) is zero.

Boundary Type:	**Mean (°C/km):**	**Median (°C/km):**	**Bin mode (°C/km) :**	**Skewness:**
Tornado-outflow	0.044	0.042	0.035 – 0.040	1.13
Hail-outflow	0.038	0.037	0.045 – 0.050	-0.41
Wind-outflow	0.033	0.033	0.030 – 0.035	-1.03
Tornado-stationary	0.041	0.040	0.060 – 0.065	-0.34
Hail-stationary	0.031	0.027	0.025 – 0.030	0.76
Wind-stationary	0.038	0.041	0.040 – 0.045	-0.64
Tornado-warm	0.042	0.045	0.040 – 0.045	-1.06
Hail-warm	0.042	0.040	0.030 – 0.035	0.076
Wind-warm	0.041	0.040	0.040 – 0.045	0.82

Table 7: List of temperature gradient distribution comparisons and associated p-values from the Two-Way KS Test. A p-value less than 0.05 means that there is less than a 5% chance that the two distributions are from the same parent distribution, and is considered statistically significant; these values are italicized below.

I. Comparisons by Boundary Type	
Distribution Comparison	**P-Value**
Tornado-Outflow and Hail-Outflow	0.0740
Tornado-Stationary and Hail-Stationary	*0.0115*
Tornado-Warm and Hail-Warm	*0.0335*
II. Comparisons by Report Type	
Distribution Comparison	**P-Value**
Tornado-Outflow and Tornado-Stationary	*0.0077*
Tornado-Outflow and Tornado-Warm	0.1026
Tornado-Stationary and Tornado-Warm	*0.0072*
Hail-Outflow and Hail-Stationary	*0.0015*
Hail-Outflow and Hail-Warm	0.3980
Hail-Stationary and Hail-Warm	*1.12e-06*

Table 8: As in Table 6, but for distance distributions, as well as with the 5-km binned mode.

Boundary Type:	**Mean (km):**	**Median (km):**	**Bin mode (km):**	**Skewness:**
Tornado-outflow	21.5	25.9	25 – 30	-0.86
Hail-outflow	17.5	24.1	30 – 35; 40 – 45	-0.58
Wind-outflow	15.8	17.4	40 – 45	-0.42
Tornado-stationary	-8.1	-15.5	-20 – (-25)	0.42
Hail-stationary	-13.7	-22.5	-25 – (-30)	0.78
Wind-stationary	-33.0	-41.2	-50 – (-55)	1.98
Tornado-warm	10.9	21.8	40 – 45	-0.62
Hail-warm	-3.0	-0.74	15 – 20	-0.13
Wind-warm	-10.2	-26.3	-40 – (-45)	0.54

Table 9: Mean and median distances (km) for significantly severe reports per boundary type. Negative distances represent the cool sector; positive distances represent the warm sector.

	Mean (km)	**Median (km)**
Tornado-outflow	21.3	37.7
Hail-outflow	9.6	10.3
Tornado-stationary	-4.5	-12.8
Hail-stationary	-5.9	-16.2
Tornado-warm	16.6	22.6
Hail-warm	-21.4	-36.7

Table 10: Total number of significantly severe reports per boundary type

	Tornado	**Hail**	**Wind**
Outflow	17	12	3
Stationary	7	44	22
Warm	29	21	1

Table 11: Ranges from the boundary for each report-boundary type that contain 67.5% of all severe weather reports. Positive distances refer to locations in the warm sector, while negative distances imply locations on the cool side of boundaries.

Distribution	**Range Containing 67.5% of Reports (km)**	**Mean Report Distance (km)**
Tornado - Outflow	-5.3 – 48.3	21.5
Hail - Outflow	-10.2 – 45.1	17.5
Tornado - Stationary	-41.1 – 25.0	-8.1

Table 12: As in Table 8, but for distributions which tested as non-normal.

	Tornado			
	Warm Sector		**Cool Sector**	
	Mean	**Range**	**Mean**	**Range**
Warm Front	29.2	14.6 – 43.9	-25.5	-43.0 - (-8.0)
	Hail			
	Warm Sector		**Cool Sector**	
	Mean	**Range**	**Mean**	**Range**
Stationary Front	34.6	20.5 - 48.6	-31.1	-44.7 - (-17.6)
Warm Front	26.7	13.7 - 39.8	-32.7	-49.6 - (-15.9)

Table 13: As in Table 7, but for report distances.

I. Comparisons by Boundary Type	
Distribution Comparison	**P-Value**
Tornado-Outflow and Hail-Outflow	0.3616
Tornado-Stationary and Hail-Stationary	0.2844
Tornado-Warm and Hail-Warm	*0.0016*
II. Comparisons by Report Type	
Distribution Comparison	**P-Value**
Tornado-Outflow and Tornado-Stationary	*1.84e-07*
Tornado-Outflow and Tornado-Warm	*3.81e-02*
Tornado-Stationary and Tornado-Warm	*5.38e-05*
Hail-Outflow and Hail-Stationary	*8.56e-12*
Hail-Outflow and Hail-Warm	*9.13e-04*
Hail-Stationary and Hail-Warm	*1.67e-04*

FIGURES

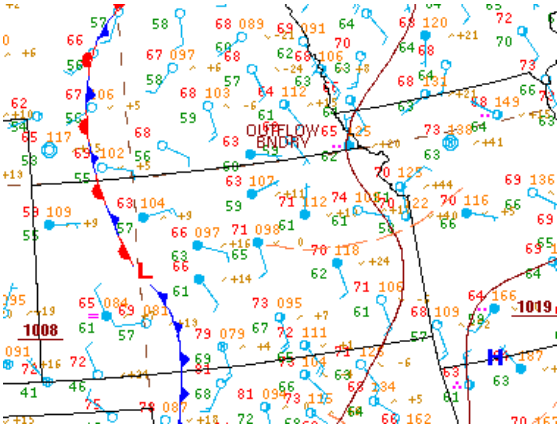

(a) 1500 UTC on May 25, 2016

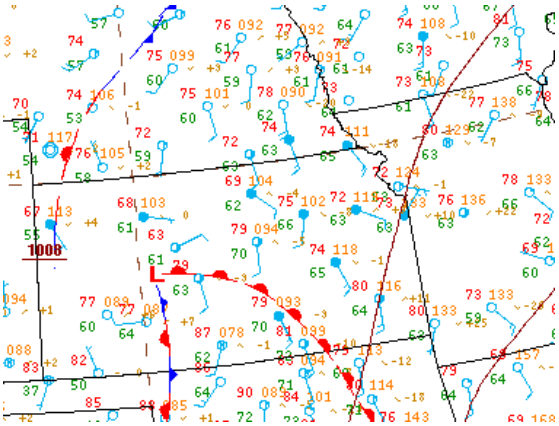

(b) 1800 UTC on May 25, 2016

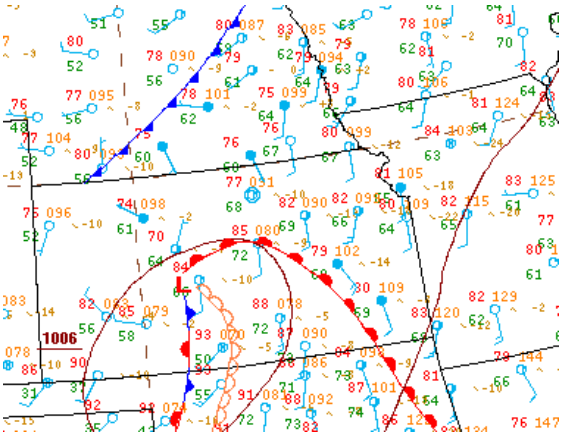

(c) 2100 UTC on May 25, 2016

Figure 1: WPC surface analysis from 25 May 2016.

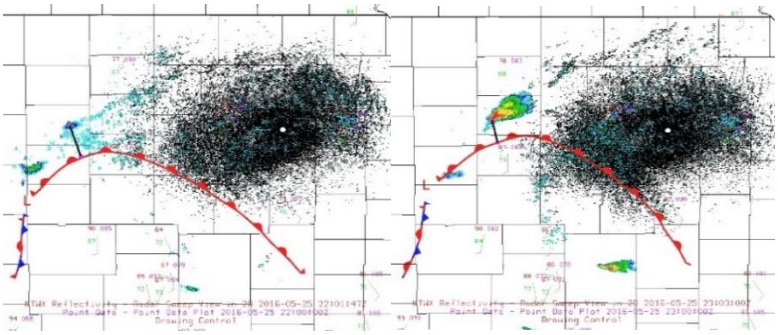

(a) 2200 UTC 25 May 2016 (b) 2300 UTC 25 May 2016

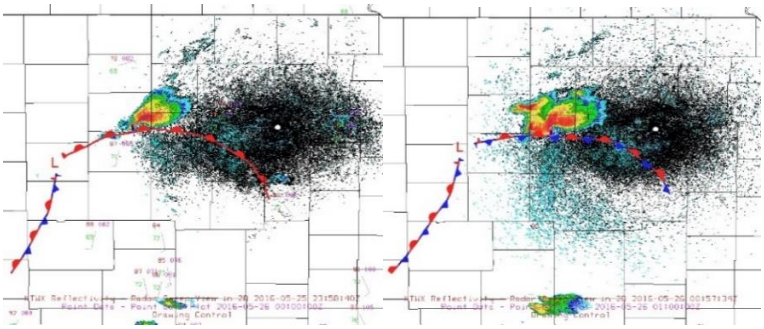

(c) 0000 UTC 26 May 2016 (d) 0100 UTC 26 May 2016

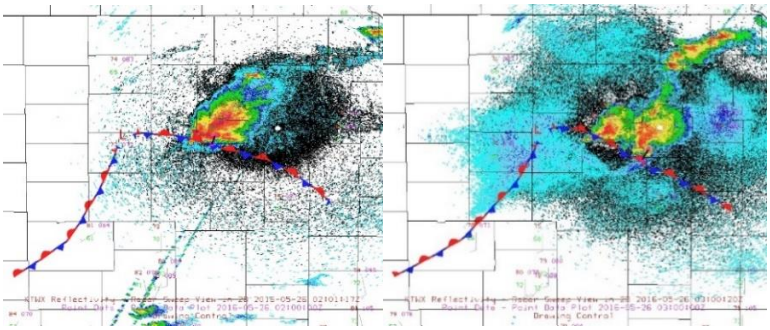

(e) 0200 UTC 26 May 2016 (f) 0300 UTC 26 May 2016

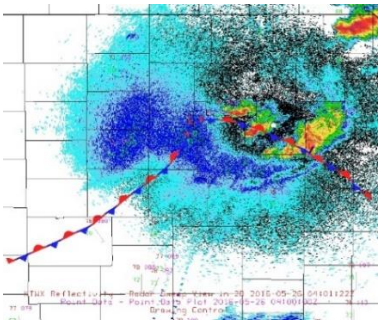

(g) 0400 UTC 26 May 2016

Figure 2: Interaction of the May 25, 2016 Kansas supercell with the warm/stationary front from 2200 to 0400 UTC. The fronts are analyzed over the radar data and ASOS archives, while the black line indicates the distance measured from the supercell to the front.

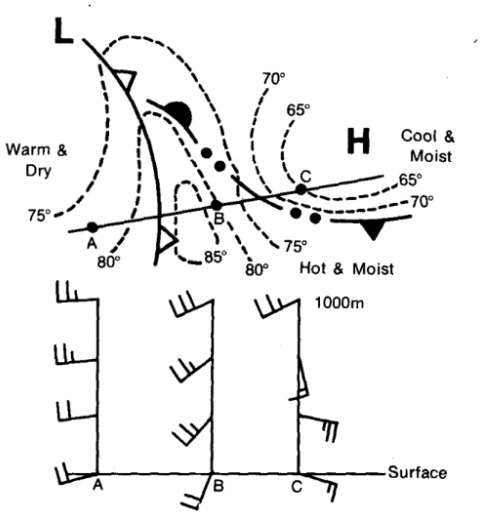

Figure 3: Cross-section through two boundaries illustrating representative wind profiles for a well-mixed warm and dry air mass (profile A), a hot and moist, conditionally unstable air mass (profile B), and a cool and moist air mass behind an outflow boundary (profile C). Figure taken from Maddox et al. (1980).

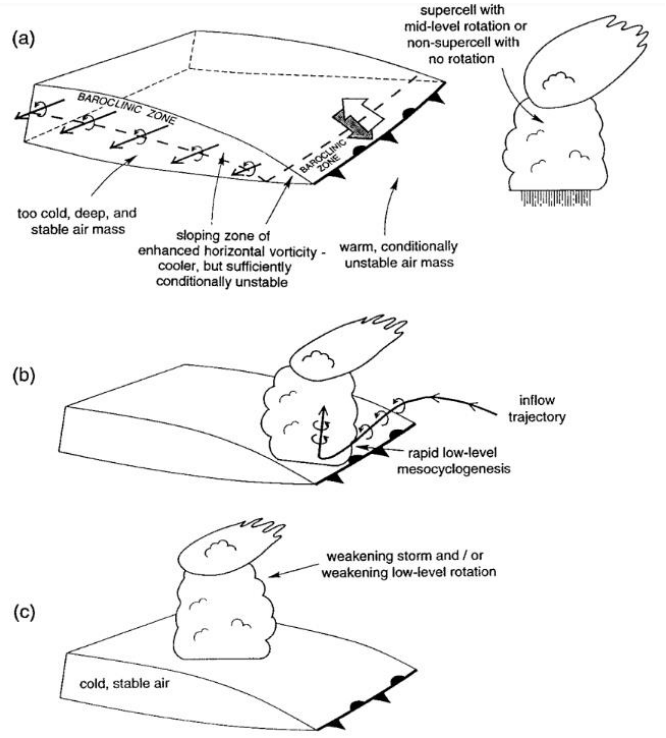

Figure 4: Conceptual model of horizontal vorticity along a baroclinic zone impacting the development of low-level rotation in a supercell. Figure from Markowski et al. (1998a).

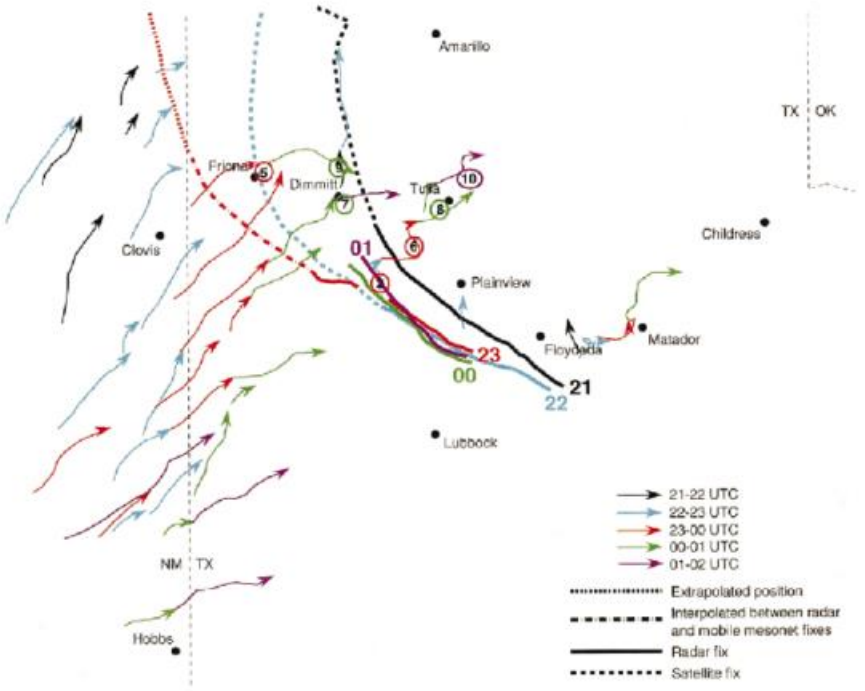

Figure 5: From Rasmussen et al. (2000), each arrow represents a storm centroid track for 5 1-hour periods depicted in the legend. The thick lines represent boundary placement at the noted times. Numbers in circles mark the occurrence of a tornado.

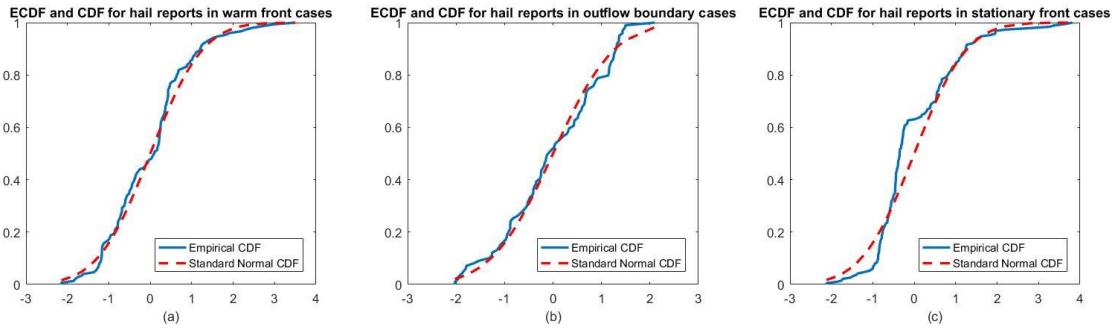

Figure 6: ECDF and CDF KS-test example for hail reports in (a) warm front cases, (b) outflow boundary cases, and (c) stationary front cases. The red dashed line represents the CDF if the data were normal. The solid blue line represents the ECDF, or the actual distribution of the data.

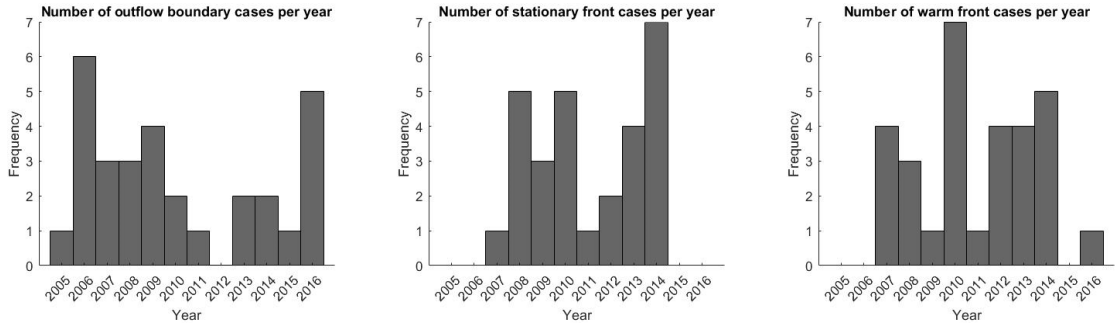

(a) (b) (c)

Figure 7: Distribution of the total number of cases per year per boundary type for outflow boundary cases (a), stationary front cases (b), and warm front cases (c).

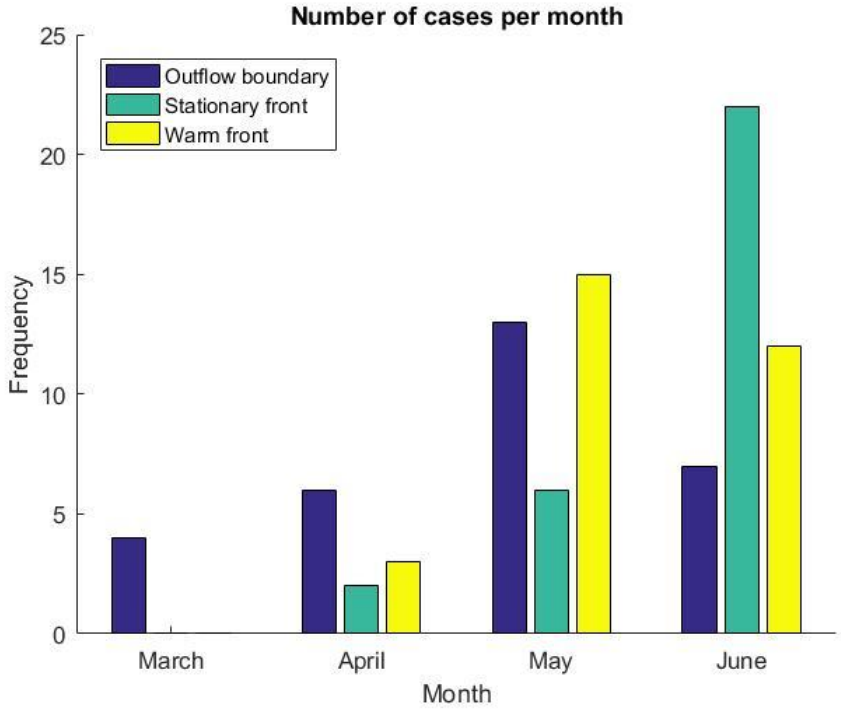

Figure 8: Distribution of total number of cases per month for outflow boundary cases (blue), stationary front cases (green), and warm front cases (yellow).

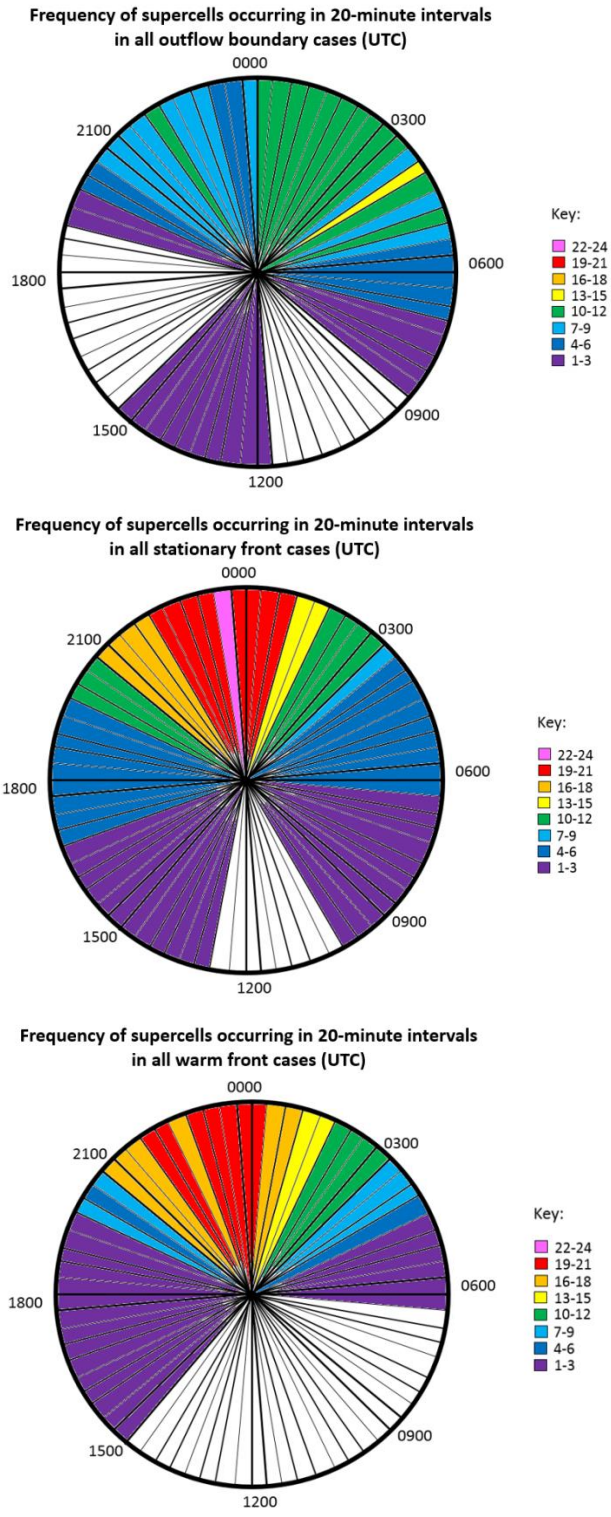

Figure 9: Time plot of how many supercells were active for each 20-minute interval in a 24-hour cycle in UTC.

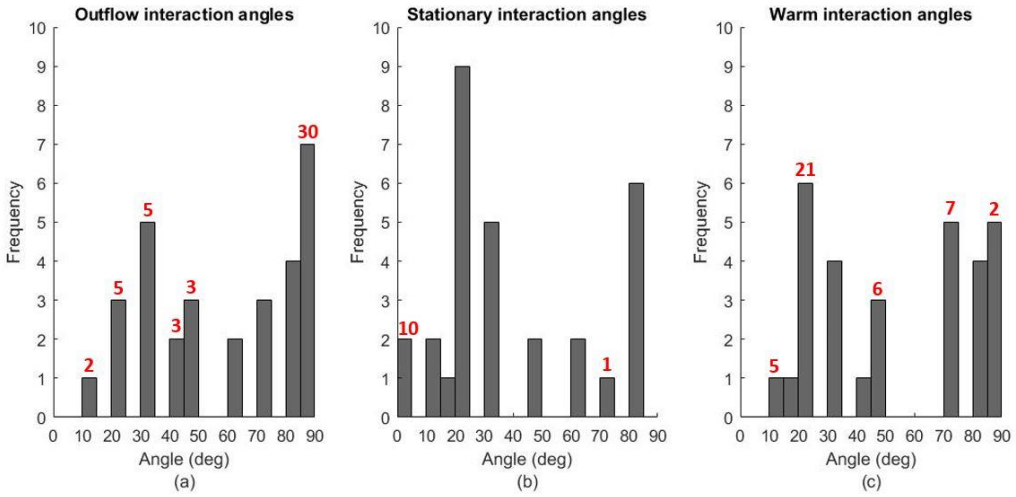

Figure 10: Histograms of supercell-boundary interaction angles for outflow (a), stationary (b), and warm fronts (c) in the black bars with frequency on the left y-axis, and the total number of significant tornadoes (>F/EF2) in the bold red text above its corresponding angle range.

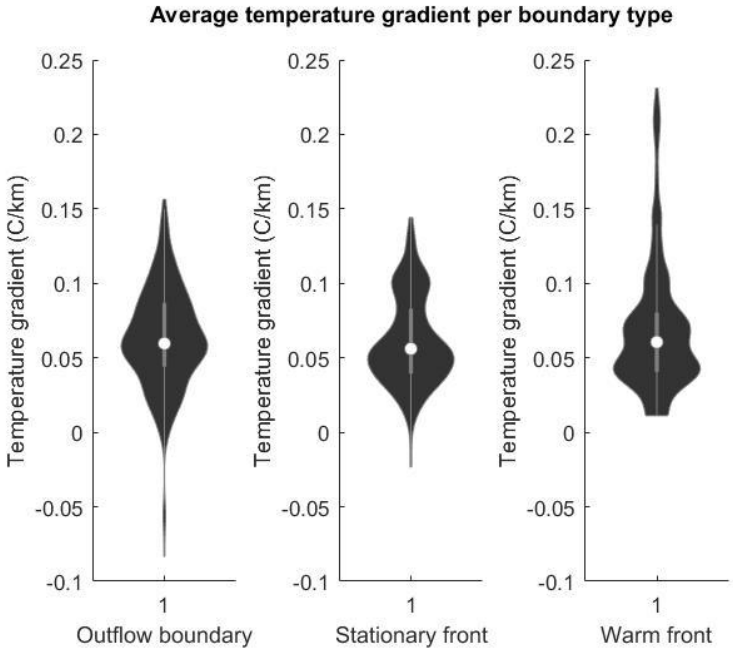

Figure 11: Violin plot of average temperature gradient of all supercells per (a) outflow boundary, (b) stationary front, and (c) warm front. The central dot marks the median, the thick grey line marks the inter-quartile range of the 25th and 75th percentiles, and the thin grey line is the range containing 95% of all data. The edges are a kernel density function of the distribution of data points, thus showing the distribution and frequency of reports rather than a traditional box plot. Negative temperature gradients are the result of the cool and warm air locations switching after the nocturnal transition.

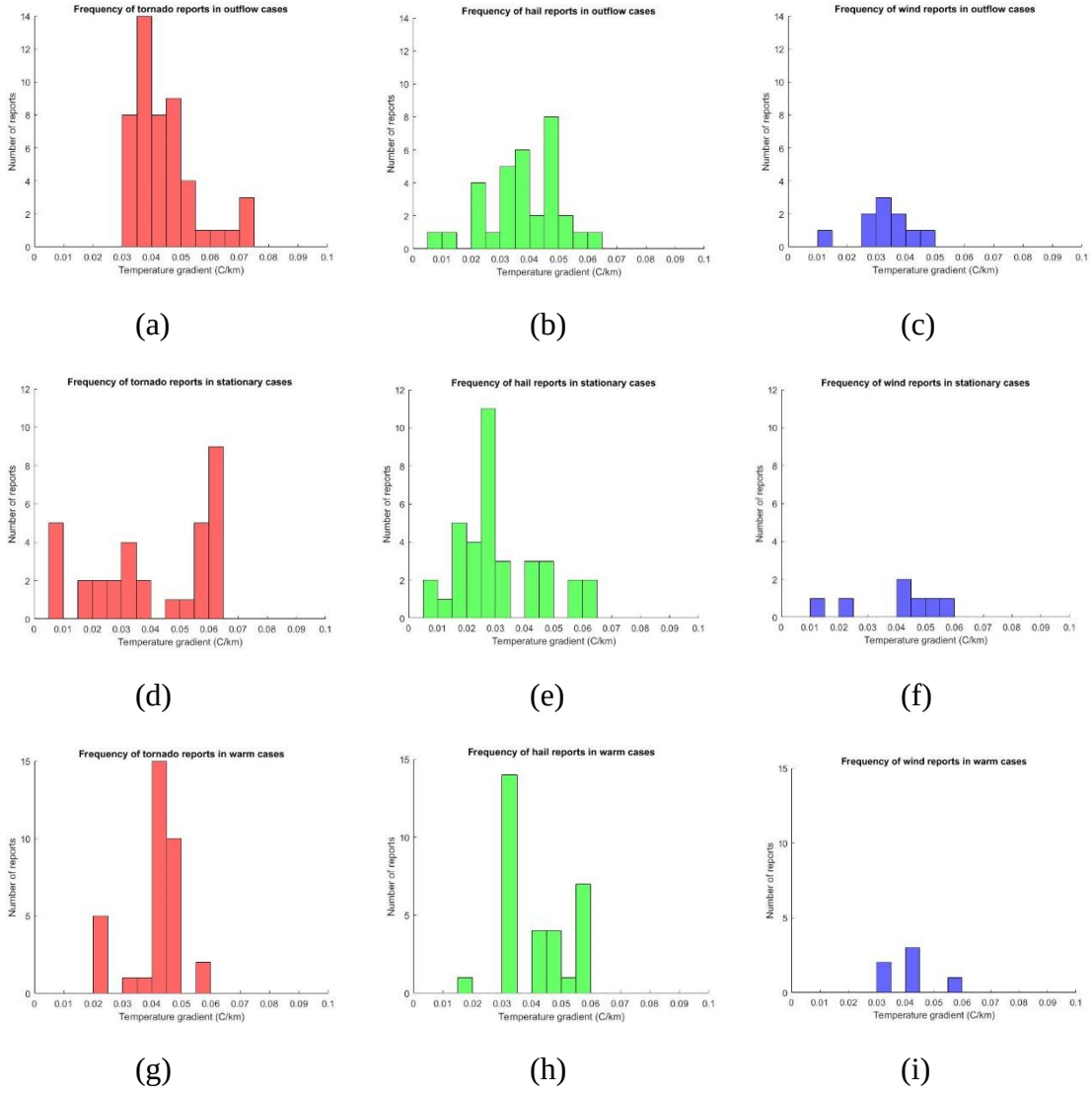

Figure 12: Histograms of temperature gradient at the time of severe reports with 0.005 °C/km bins.

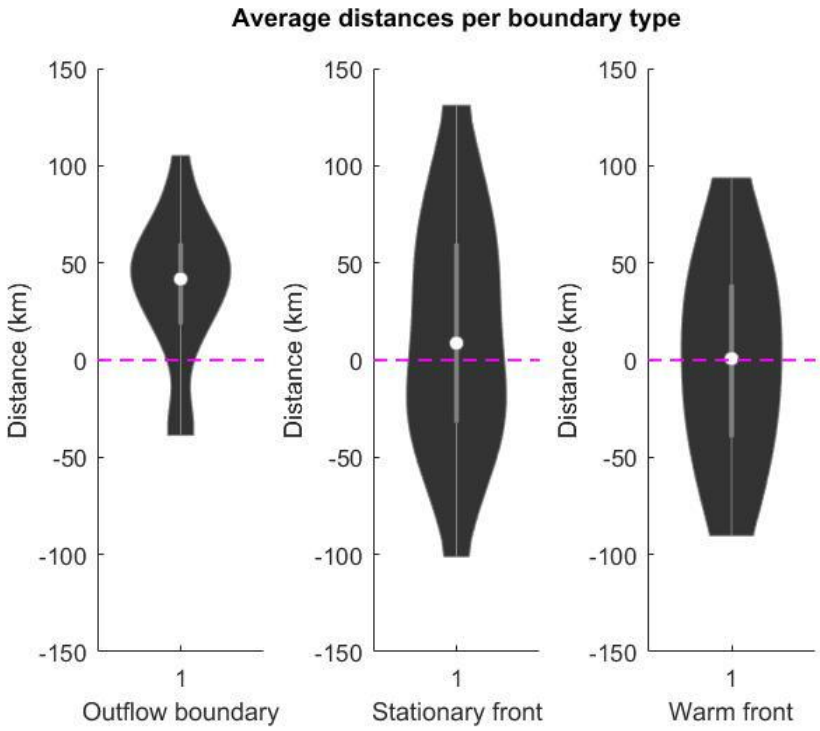

Figure 13: As in Fig. 11, but for average distance of all supercells per boundary type, where the boundary is indicated by the value 0. Positive distances represent the warm sector and negative values represent the cool sector. Boundary denoted by the magenta dashed line.

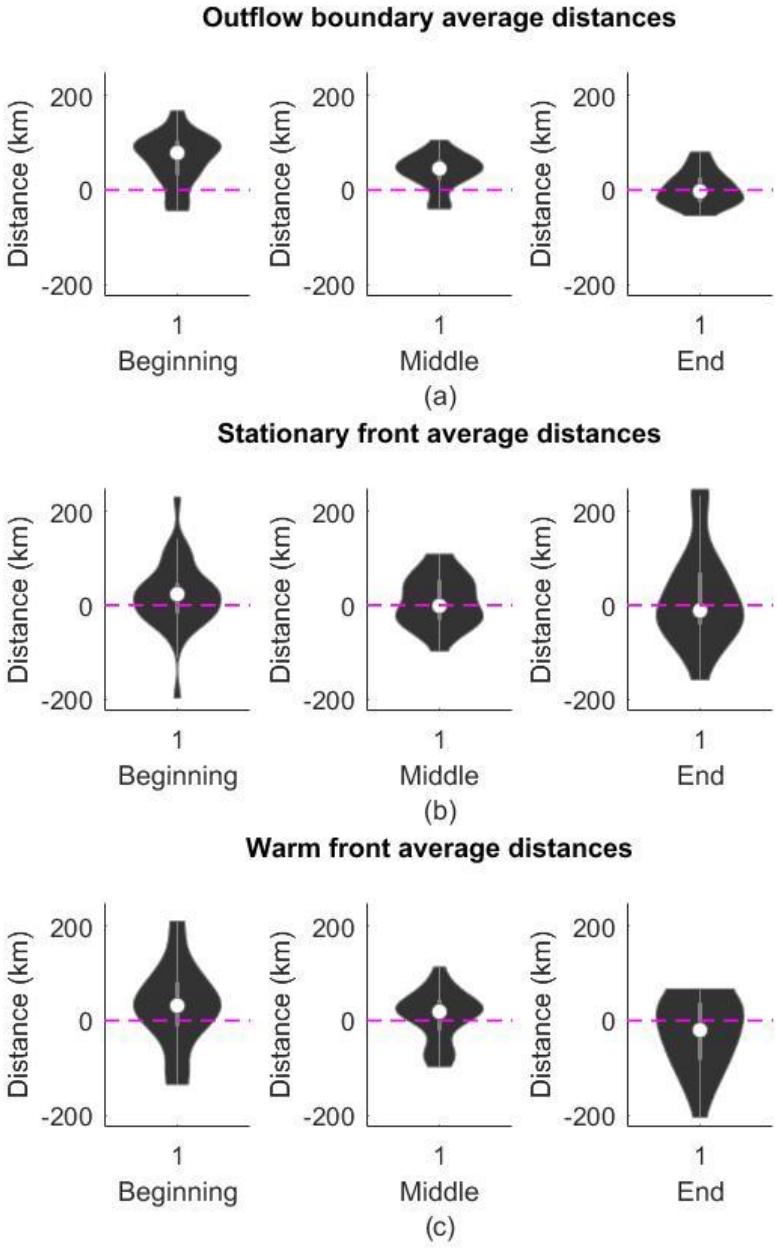

Figure 14: Violin plots with the mean distances of supercells interacting with an outflow boundary (top), stationary front (middle), or warm front (bottom) at the beginning, middle, and end of their lifetimes. Plot features as in Fig. 11. Boundary location denoted by the magenta dashed line.

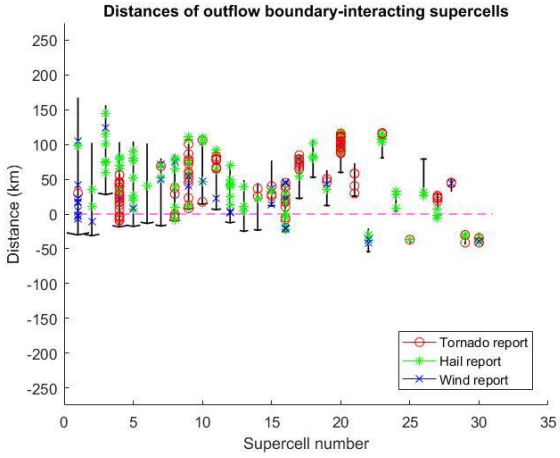
Distances of outflow boundary-interacting supercells
Distance (km)
Supercell number
Tornado report
Hail report
Wind report

(a)

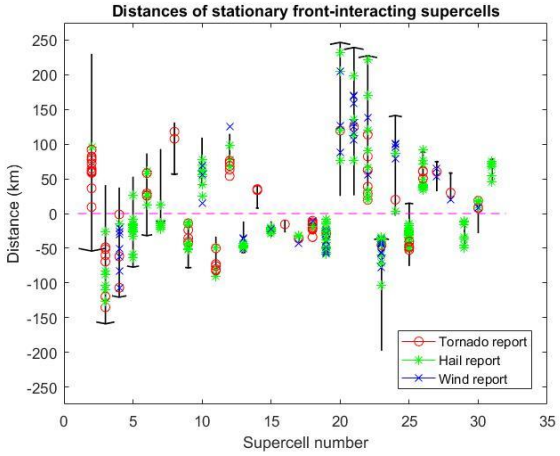
Distances of stationary front-interacting supercells
Distance (km)
Supercell number
Tornado report
Hail report
Wind report

(b)

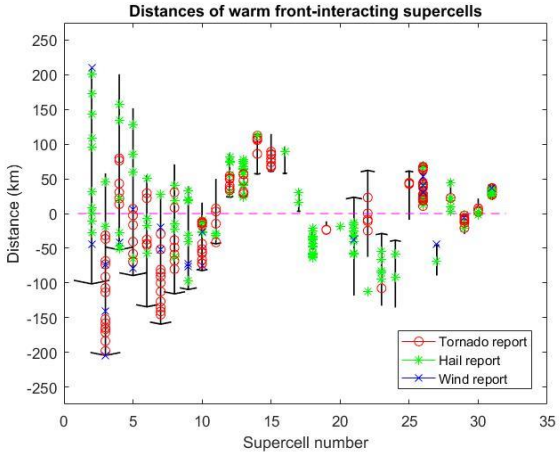
Distances of warm front-interacting supercells
Distance (km)
Supercell number
Tornado report
Hail report
Wind report

(c)

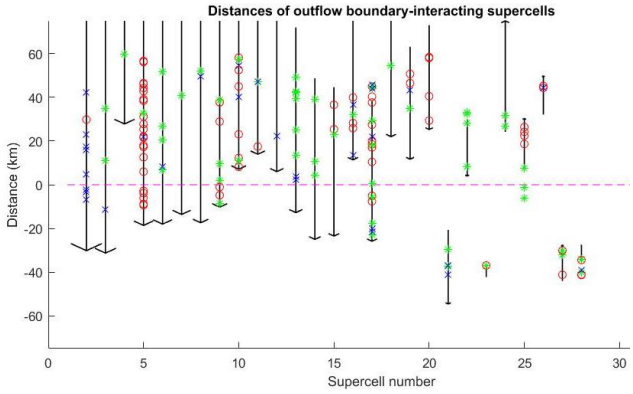

(d)

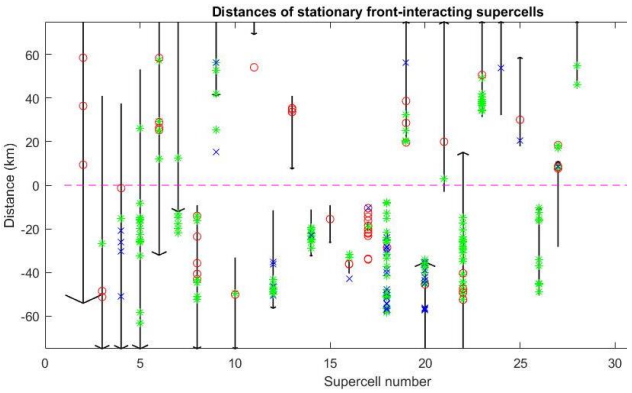

(e)

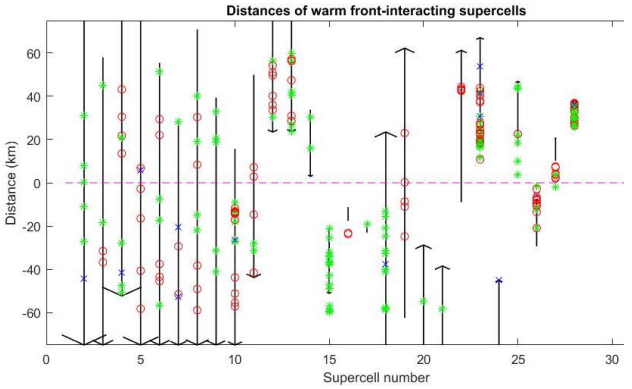

(f)

Figure 15: Supercell motion vectors starting at boundary distance at the beginning of the supercell's lifetime and ending at the end of the supercell's lifetime for (a) outflow boundary-interacting supercells, (b) stationary front-interacting supercells, and (c) warm front-interacting supercells. Negative distances correlate to supercell location in the cool sector. The y-axis represents the distance from the boundary (purple-dashed line) with distances in the warm sector as a positive distance, and distances in the cool sector as a negative distance. The vectors are separated by direction of supercell motion towards warmer or cooler air, and then sorted by total path difference within those two sectors. Vectors which appear very small traveled along the boundary, resulting in a smaller total path difference. These vectors extend from the supercell's starting distance from the boundary to its ending distance. Zoomed in plots are in figures (d), (e), and (f) for outflow, stationary, and warm fronts, respectively, with cases limited by 60 km.

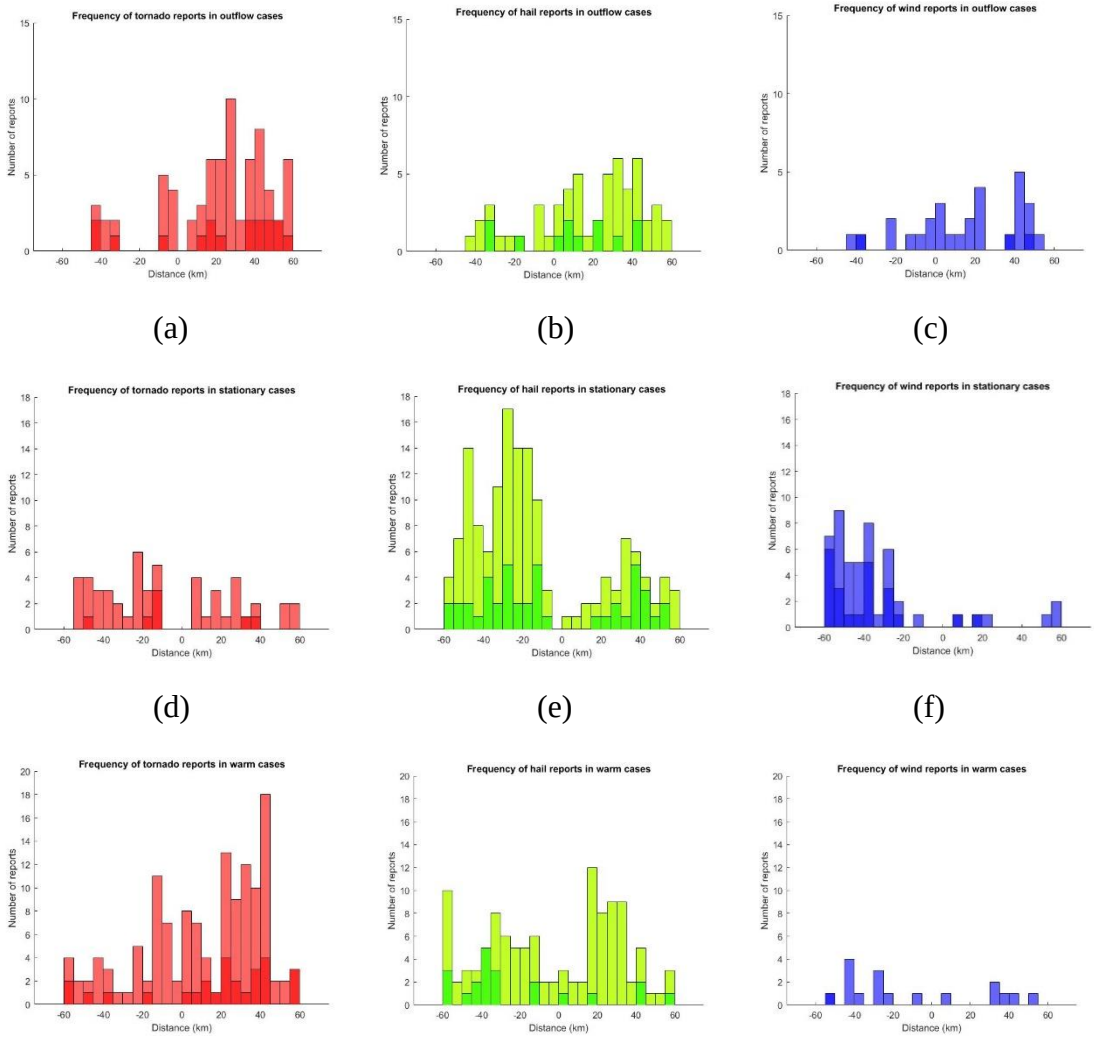

Figure 16: Histograms of distance of severe report for the three boundaries with 5 km bins with the significantly severe reports distributions marked in the darker colors.

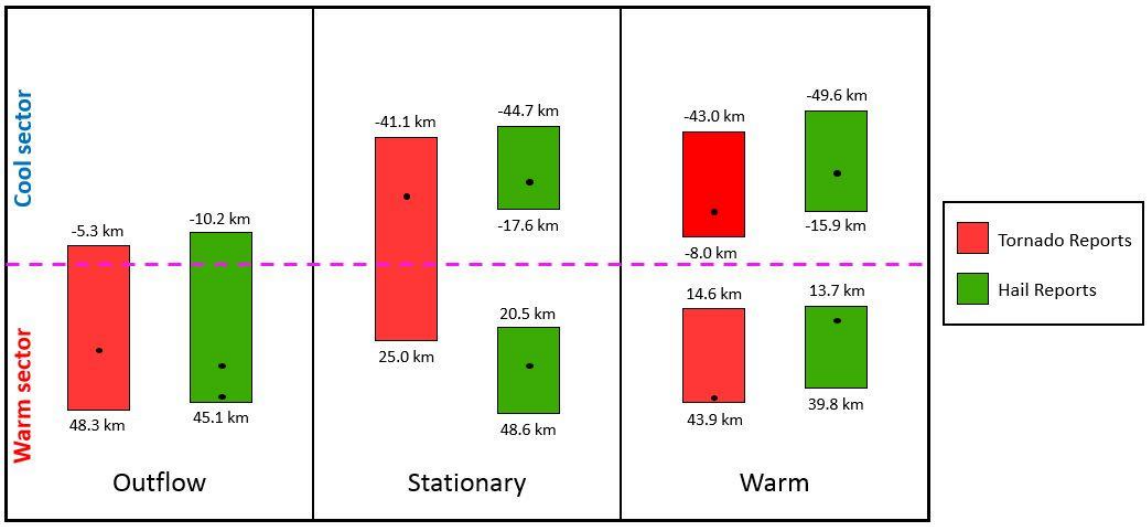

Figure 17: Visual representation of the distances that contain one standard deviation around the mean distance from the boundary (dashed magenta line) for each storm report type per boundary type (+/- 10 km). Negative distances indicate distance is in the cool sector, positive distances are the warm sector. Black dot represents mode of the distribution. (Note: the hail-outflow distribution has two modes).